Astron. Astrophys. 335, 403–420 (1998)

ASTRONOMY AND ASTROPHYSICS

The chemistry of the early Universe

Daniele Galli and Francesco Palla

Osservatorio Astrofisico di Arcetri, Largo E. Fermi 5, I-50125 Firenze, Italy

Received 4 November 1997 / Accepted 31 March 1998

Abstract. The process of molecule formation in the primordial gas is considered in the framework of Friedmann cosmological models from redshift $z = 10^4$ to $z = 0$. First, a comprehensive analysis of 87 gas phase reaction rates (both collisional and radiative) relevant in the physical environment of the expanding universe is presented and critically discussed. On this basis, calculations are carried out of the abundance of 21 molecular species as function of redshift, for different values of the cosmological parameters Ω_0, η and H_0, evaluating consistently the molecular heating and cooling due to H_2, HD and LiH molecules. One of the major improvements of this work is the use of a better treatment of H recombination that leads to a reduction of a factor 2–3 in the abundance of electrons and H^+ at freeze-out, with respect to previous studies. The lower residual ionization has a negative effect on the chemistry of the primordial gas in which electrons and protons act as catalysts in the formation of the first molecules. We find that in the standard model ($h = 0.67$, $\eta_{10} = 4.5$, $\Omega_0 = 1$ and [D/H] $= 4.3 \times 10^{-5}$), the residual fractional ionization at $z = 1$ is $[\mathrm{e/H}] = 3.02 \times 10^{-4}$, and the main molecular species fractional abundances $[\mathrm{H_2/H}] = 1.1 \times 10^{-6}$, $[\mathrm{HD/H_2}] = 1.1 \times 10^{-3}$, $[\mathrm{HeH^+/H}] = 6.2 \times 10^{-13}$, $[\mathrm{LiH^+/H}] = 9.4 \times 10^{-18}$ and $[\mathrm{LiH/LiH^+}] = 7.6 \times 10^{-3}$. We devise a reduced chemical network that reproduces with excellent accuracy the numerical results of the complete model and allows to follow the chemical compositions and the thermal properties of a primordial gas in the presence of an external radiation field. Finally, we provide accurate cooling functions of H_2, HD and LiH in a wide range of density and temperature that can be conveniently used in a variety of cosmological applications.

Key words: molecular processes – atomic processes – early Universe

1. Introduction

The study of molecule formation in the post-recombination epoch has grown considerably in recent years. Saslaw & Zipoy (1967) and Peebles & Dicke (1968) were the first to realize the importance of gas phase reactions for the formation of the simplest molecule, H_2. They showed that trace amounts of molecular hydrogen, of order 10^{-6}–10^{-5}, could indeed form via the intermediaries species H_2^+ and H^- once the radiation field no longer contained a high density of photons with energies above the threshold of dissociation (2.64 and 0.75 eV, respectively).

The presence of even a trace abundance of H_2 is of direct relevance for the cooling properties of the primordial gas which, in its absence, would be an extremely poor radiator: cooling by Ly-α photons is in fact ineffective at temperatures $\lesssim 8000$ K, well above the matter and radiation temperature in the post-recombination era. Since the evolution of primordial density fluctuations is controlled by the ability of the gas to cool down to low temperatures, it is very important to obtain a firm picture of the chemistry of the dust-free gas mixture, not limited to the formation of H_2, but also to other molecules of potential interest. In this regard, Lepp & Shull (1984) and Puy et al. (1993) have computed the abundances of H_2, HD and LiH as a function of redshift for various cosmological models. Although the final abundances of H_2 and HD agree in the two calculations, their evolution with redshift is markedly different, since the epoch of formation varies by a factor of ~ 2. Also, the LiH abundance shows a large discrepancy of about two orders of magnitude.

More recently, Palla et al. (1995) have analyzed the effects on the chemistry of the pregalactic gas of a high primordial D abundance in the light of the controversial results obtained towards high redshift quasars (see e.g. Tytler & Burles 1997). They found that the abundance of H_2 is rather insensitive to variations in the cosmological parameters implied by a factor of ~ 10 enhancement of primordial [D/H], while HD and LiH abundances vary by larger amounts. However, the abundance of LiH, obtained with simple estimates of the radiative association rate, was largely overestimated. Because of the potential relevance of the interaction of LiH molecules with the cosmic background radiation (CBR) (Maoli et al. 1994), a proper treatment of the lithium chemistry was necessary. Dalgarno et al. (1996) and Gianturco & Gori Giorgi (1996a,b) provided accurate quantum-mechanical calculations of the main reaction rates. The chemistry of lithium in the early universe has been then studied by Stancil et al. (1996) and Bougleux & Galli (1997). Finally, useful reviews of the chemistry of the early universe can be found in Dalgarno & Lepp (1987), Black (1991), Shapiro (1992), and

Send offprint requests to: D. Galli, (galli@arcetri.astro.it)

Abel et al. (1997). The latter two studies, in particular, focus on the nonequilibrium H_2 chemistry in radiative shocks which is thought to be of primary importance during the gravitational collapse of density fluctuations (see also Anninos et al. 1997).

In spite of such a wealth of specific studies, a comprehensive analysis of the subject and a critical discussion of the reaction paths and rates are still lacking. To overcome this limitation, in this paper we present a complete treatment of the evolution of *all* the molecular and atomic species formed in the uniform pregalactic medium at high redshifts ($z < 10^4$). The structure of the paper is as follows: in Sect. 2 we describe the H, D, He, and Li chemistry, with a critical discussion of the most important rates; the evolutionary models are presented in Sect. 3, and the results for the standard model and the dependence on the cosmological parameters are given in Sect. 4; Sect. 5 introduces a minimal model which highlights the dominant reactions for the formation of H_2, HD, HeH^+, LiH and LiH^+; a comparison with the results of previous studies is given in Sect. 6, and the conclusions are summarized in Sect. 7. Also, the Appendix provides the collisional excitation coefficients for HD and H_2 and cooling function of H_2, HD and LiH which are needed for the computation of the thermal evolution of the primordial gas.

2. The chemical network

The chemical composition of the primordial gas consists of e^-, H, H^+, H^-, D, D^+, He, He^+, He^{++}, Li, Li^+, Li^-, H_2, H_2^+, HD, HD^+, HeH^+, LiH, LiH^+, H_3^+, and H_2D^+. The fractional abundaces of these species are calculated as function of redshift, starting at $z = 10^4$ where He, H, D, and Li are fully ionized. The network includes 87 reactions with the rate coefficients taken from the most recent theoretical and experimental determinations. Reactions rates are listed separately for each atomic element in Tables 1 to 4. In each table, column 2 gives the reaction, and column 3 the rate coefficient (in cm^3 s^{-1} for collisional processes, in s^{-1} for photo-processes). The gas and radiation temperatures are indicated by $T_{\rm g}$ and $T_{\rm r}$, respectively. The temperature range of validity of the rate coefficients and remarks on the rate are given in column 4, together with some remarks on how the rate was obtained. When reaction rates were not available, we have integrated the cross sections and fitted the results with simple analytical expressions (generally accurate to within 10%). The last column gives the reference for the rate or the cross section adopted.

The assessment of the accuracy of each rate while in principle extremely valuable, is hampered by the large number of reactions considered. In this work, we prefer to limit the discussion to those rates that are critical for a correct estimate of the final molecular abundances, without omitting any important process. In doing so, we will consider the reactions that enter in what will be called below the *minimal model*, i.e. the reduced set of processes that are needed to compute the evolution of the main molecular species H_2, H_2^+, HD, HeH^+, LiH and LiH^+. In particular, for hydrogen we compare our rates to those used by Abel et al. (1997) in their extensive compilation. For D, He and Li we will refer to rates found in the literature as well as in databases. For ease of comparison, we show the data from experiments/theory, our numerical fit, and the rates adopted by other authors in Fig. 1 for H, in Fig. 2 for D and He, and in Fig. 3 for Li. In this way, one can immediately appreciate the degree of uncertainty associated with each rate.

2.1. Hydrogen chemistry

(H1)-(H2) H recombination

The process of cosmological recombination has been analyzed in detail in a number of studies, most recently by Jones & Wyse (1985), Krolik (1990), Grachev & Dubrovich (1991), and Sasaki & Takahara (1993). The improved treatment of stimulated processes during recombination followed by the last two goups has led to a more accurate estimate of the electron abundance at freeze-out. Compared to the results of Jones & Wyse (1985) the residual ionization degree is a factor 2–3 lower, depending on the cosmological model. Of course, the reduced number of free electrons and protons has a direct effect on the chemical evolution of the gas. In this paper we have solved the full equation for the time evolution of the electron abundance (Eq. (1) of Sasaki & Takahara 1993) using the prescriptions for the rate of radiative recombination given by Grachev & Dubrovich (1991). In practice, the value for the rate of radiative transition from the continuum to the excited states is given by the simple power-law fit $R_{c2} = 8.76 \times 10^{-11}(1+z)^{-0.58}$ cm^3 s^{-1}. The inverse rate from the excited levels to the continuum is $R_{2c} = 2.41 \times 10^{15} T_{\rm r}^{1.5} \exp(-39472/T_{\rm r}) R_{c2}$ s^{-1}.

(H3) Radiative attachement of H

We have fitted the data tabulated by de Jong (1972) (triangles), based on the cross section of Ohmura & Ohmura (1960). As seen in Fig. 1, our fit (solid line) agrees well with the expression used by Abel et al. (1997) (dashed line).

(H4) Radiative detachment of H^-

The cross section for this reaction is known with great accuracy (Wishart 1979). We compare in Fig. 1 our fit (solid line) to the the rate tabulated by de Jong (1972) (triangles). The expression given by Tegmark et al. (1997) is shown by a dashed line.

(H5) Associative detachment of H and H^-

There is substantial agreement between the value of this rate coefficient (to within $\sim 10\%$) at temperatures below $\sim 10^3$ K and the experimental measurement at $T = 300$ K performed by Schmeltekopf et al. (1967). At higher temperatures earlier results by Browne & Dalgarno (1969) indicated a slow rise in the value of the rate, whereas the more recent calculations of Launay et al. (1991) show a significant decline. An uncertainty of about 50 %, however, is still present in the data due to the uncertainty on the interaction potential. Our fit (solid line in Fig. 1) is based on the results by Launay et al. (1991), and is in reasonable agreement with the fit of Shapiro & Kang (1987)

Table 1. Reaction rates for Hydrogen species

	reaction	rate (cm^3 s^{-1} or s^{-1})	notes	reference
H1)	$\mathbf{H^+ + e \rightarrow H + \gamma}$	R_{c2}	see text	
H2)	$\mathbf{H + \gamma \rightarrow H^+ + e}$	R_{2c}	see text	
H3)	$\mathbf{H + e \rightarrow H^- + \gamma}$	$1.4 \times 10^{-18} T_{\rm g}^{0.928} \exp\left(-\frac{T_{\rm g}}{16200}\right)$	fit	DJ
H4)	$\mathbf{H^- + \gamma \rightarrow H + e}$	$1.1 \times 10^{-1} T_{\rm r}^{2.13} \exp\left(-\frac{8823}{T_{\rm r}}\right)$	fit	DJ
H5)	$\mathbf{H^- + H \rightarrow H_2 + e}$	1.5×10^{-9}	$T_{\rm g} \leq 300$	
		$4.0 \times 10^{-9} T_{\rm g}^{-0.17}$	$T_{\rm g} > 300$, fit	LDZ
H6)	$H^- + H^+ \rightarrow H_2^+ + e$	$6.9 \times 10^{-9} T_{\rm g}^{-0.35}$	$T_{\rm g} \leq 8000$	
		$9.6 \times 10^{-7} T_{\rm g}^{-0.9}$	$T_{\rm g} > 8000$, fit	Po
H7)	$\mathbf{H^- + H^+ \rightarrow 2H}$	$5.7 \times 10^{-6} T_{\rm g}^{-0.5} + 6.3 \times 10^{-8} -$		
		$9.2 \times 10^{-11} T_{\rm g}^{0.5} + 4.4 \times 10^{-13} T_{\rm g}$	fit by PAMS	MAP
H8)	$\mathbf{H + H^+ \rightarrow H_2^+ + \gamma}$	$\mathrm{dex}[-19.38 - 1.523 \log T_{\rm g} +$		
		$1.118 (\log T_{\rm g})^2 - 0.1269 (\log T_{\rm g})^3]$	$1 \leq T_{\rm g} \leq 32000$, fit	RP, SBD
H9)	$\mathbf{H_2^+ + \gamma \rightarrow H + H^+}$	$2.0 \times 10^1 T_{\rm r}^{1.59} \exp\left(-\frac{82000}{T_{\rm r}}\right)$	$v = 0$, fit	Du
		$1.63 \times 10^7 \exp\left(-\frac{32400}{T_{\rm r}}\right)$	LTE, fit	Ar, St
H10)	$\mathbf{H_2^+ + H \rightarrow H_2 + H^+}$	6.4×10^{-10}		KAH
H11)	$H_2^+ + e \rightarrow 2H$	$2.0 \times 10^{-7} T_{\rm g}^{-0.5}$	$v = 0$, fit	SDGR
H12)	$H_2^+ + \gamma \rightarrow 2H^+ + e$	$9.0 \times 10^1 T_{\rm r}^{1.48} \exp\left(-\frac{335000}{T_{\rm r}}\right)$	fit	BO
H13)	$H_2^+ + H_2 \rightarrow H_3^+ + H$	2.0×10^{-9}		TH
H14)	$H_2^+ + H \rightarrow H_3^+ + \gamma$	irrelevant		KH
H15)	$\mathbf{H_2 + H^+ \rightarrow H_2^+ + H}$	$3.0 \times 10^{-10} \exp\left(-\frac{21050}{T_{\rm g}}\right)$	$T_{\rm g} \leq 10^4$, fit	
		$1.5 \times 10^{-10} \exp\left(-\frac{14000}{T_{\rm g}}\right)$	$T_{\rm g} > 10^4$, fit	HMF
H16)	$H_2 + e \rightarrow H + H^-$	$2.7 \times 10^{-8} T_{\rm g}^{-1.27} \exp\left(-\frac{43000}{T_{\rm g}}\right)$	$v = 0$, fit	SA
H17)	$H_2 + e \rightarrow 2H + e$	$4.4 \times 10^{-10} T_{\rm g}^{0.35} \exp\left(-\frac{102000}{T_{\rm g}}\right)$	fit by MD	Co
H18)	$H_2 + \gamma \rightarrow H_2^+ + e$	$2.9 \times 10^2 T_{\rm r}^{1.56} \exp\left(-\frac{178500}{T_{\rm r}}\right)$	fit	OR
H19)	$H_3^+ + H \rightarrow H_2^+ + H_2$	$7.7 \times 10^{-9} \exp\left(-\frac{17560}{T_{\rm g}}\right)$	fit	SMT
H20)	$H_3^+ + e \rightarrow H_2 + H$	$4.6 \times 10^{-6} T_{\rm g}^{-0.65}$		Su
H21)	$H_2 + H^+ \rightarrow H_3^+ + \gamma$	1.0×10^{-16}		GH
H22)	$H_3^+ + \gamma \rightarrow H_2^+ + H$	irrelevant		KH

Ar: Argyros (1974); BO: Bates & Opik (1968); Co: Corrigan (1965); DJ: de Jong (1972) ; Du: Dunn (1968) ; GH: Gerlich & Horning (1992) ; HMF: Holliday et al. (1971) ; KAH: Karpas et al. (1979); KH: Kulander & Heller (1978); LDZ: Launay et al. (1991); MAP: Moseley et al. (1970) ; MD: Mitchell & Deveau (1983); OR: ONeil & Reinhardt (1978); PAMS: Peterson et al. (1971); Po: Poulaert et al. (1978); RP: Ramaker & Peek (1976); SA: Schulz & Asundi (1967); SBD: Stancil et al. (1993); SDGR: Schneider et al. (1994); SMT: Sidhu et al. (1992); St: Stancil (1994) Su: Sundström et al. (1994); TH: Theard & Huntress (1974)

to the data of Bieniek (1980). On the other hand, Abel et al. (1997) favor a rate increasing with temperature for $T > 1000$ K, assuming a rate based on the cross section of Browne & Dalgarno (1969).

(H7) Mutual neutralization of H^- and H^+

This rate is still subject to large uncertainties at low temperatures ($T \lesssim 2000$ K). Our fit in Fig. 1 (solid line) is based on the cross sections of Peterson et al. (1971) and Moseley et al. (1970) and the experimental point at $T = 300$ K of Moseley et al. (1970). At temperatures below $\sim 10^3$ K, we have extrapolated as a power-law ($\propto E^{-1}$) the cross section of Moseley et al. (1970). The rate used by Abel et al. (1997) is the same as Dalgarno & Lepp (1987) and it is shown by the long-dashed line. Finally, the rate adopted by Shapiro & Kang (1987), taken from Duley & Williams (1984), is shown by the dashed line.

(H8) Radiative association of H and H^+

This reaction rate has been computed quantum-mechanically by Ramaker & Peek (1976) and more recently by Stancil et al. (1993). The two calculations agree to within 3% from $T = 10$ K up to $T = 10^6$ K. In Fig. 1 we show the values tabulated by Ramaker & Peek (1976) (triangles), our polynomial fit (solid line), and the fit by Abel et al. (1997) (dashed line) taken from Shapiro & Kang (1987). Since this reaction is important at large redshifts when the temperature is well above $\sim 10^3$ K, the departure of the fit at low T is of little consequence on the final H_2 abundances.

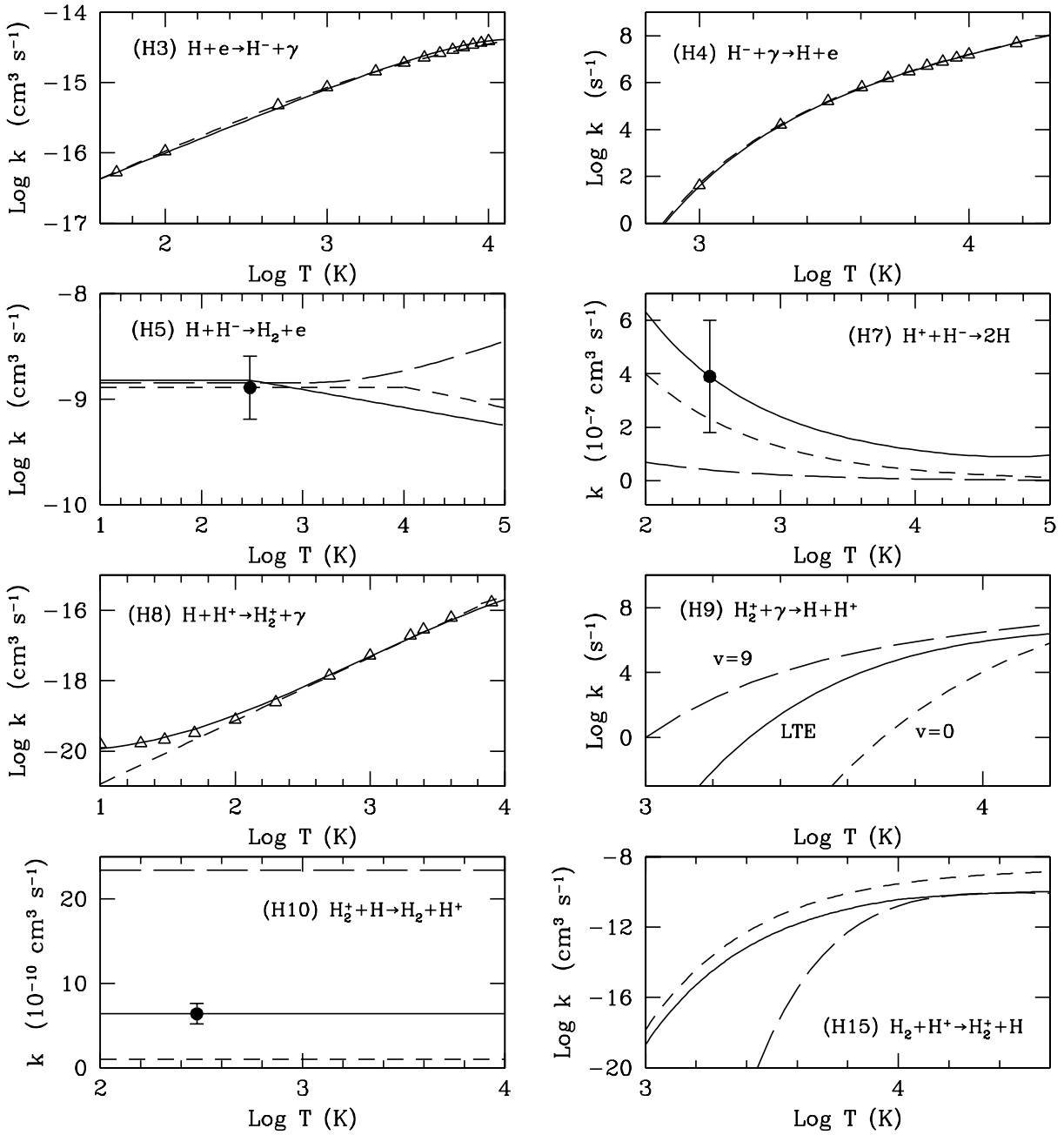

Fig. 1. Rate coefficients for H_2 chemistry.

(H9) Photodissociation of H_2^+

The evolution of H_2^+, and, to a large extent, that of H_2 depend crucially on the rate of this reaction. Unfortunately, calculations of the photodissociation cross section are available only for a sparse set of vibrational levels (Dunn 1968, Argyros 1974). Total cross sections, averaged over a LTE distribution of level populations, have been computed by Argyros (1974) for $2500\ \mathrm{K} < T < 26000\ \mathrm{K}$ and by Stancil (1994) for $3150\ \mathrm{K} < T < 25200\ \mathrm{K}$. The theoretical calculations are in excellent agreement and reproduce satisfactorily well the experimental results by von Busch & Dunn (1972). In Fig. 1 we show the LTE photodissociation rate (solid line), compared with the rates for photodissociation from the $v = 0$ and $v = 9$ levels (dashed and long-dashed lines, respectively). In our standard model we adopt the LTE value, but we also show the sensitivity of the results to other choices of the reaction rate.

(H10) H_2 formation via H_2^+

As in most other studies, we assume a rate independent of temperature, corresponding to the measurement at $T = 300$ K by Karpas et al. (1979). The Langevin rate is shown by the long-dashed line. An uncertainty of a factor of ~ 6 is still present

in the literature as indicated by the dashed line in Fig. 1 (Culhane & McCray 1995). Such a reduction only affects the final H_2^+ abundance by almost the same factor, while leaves the H_2 abundance unchanged within a few percent.

(H15) Charge exchange of H_2 with H^+

We have integrated the cross section measured by Holliday et al. (1971) and our fit is shown by the solid line. The dashed line shows the rate used by Shapiro & Kang (1987), based on a simple detailed balance from the reverse reaction. The rate computed by Abel et al. (1997) from the calculations of Janev et al. (1987) shows a dramatic drop at $T < 10^4$ K (long dashed line in Fig. 1). However, Janev et al.'s (1987) data are accurate only for T higher than $\sim 10^4$ K, and should be disregarded at lower temperatures. In any case, as noted by Abel et al. (1997), large differences in this range of temperatures do not affect significantly the final abundances of H_2 and H_2^+.

2.2. Deuterium chemistry

(D1)-(D2) D recombination and ionization

These processes have been treated in the same way as hydrogen (see (H1) and (H2)).

(D3)-(D4) Charge exchange of D and H

These reactions control the evolution of D^+. For (D3) we have fitted the tabulated rate coefficient of Watson et al. (1978) which shows a weak temperature dependence. The rate coefficient for the reverse reaction (D4) is obtained by multiplying the direct one by $\exp(43/T)$. The fit is shown in Fig. 2 together with the data by Watson et al. (1978) (triangles). Puy et al. (1993) assume a constant rate that differs from ours by a factor of 2 in the temperature interval 10–1000 K.

(D8) Formation of HD via H_2

We have used a rate equal to the Langevin collision rate constant (solid line in Fig. 2). This rate is slightly bigger (2.1×10^{-9} vs. 1.7×10^{-9}) than the experimental result of Smith et al. (1982) at $T = 205$ K, but well in agreement at $T = 300$ K (filled circles). These values are larger than the previous measurements by Fehsenfeld et al. (1973) (filled triangles) and the theoretical estimate by Gerlich (1982).

(D10) Destruction of HD via H^+

This is the reverse reaction of (D8) which is endoergic by 464 K. The solid line in Fig. 2 is the rate given by Smith et al. (1982). The dashed line is the theoretical result by Gerlich (1982). The data points at $T = 205$ and 295 K are from Henchmann et al. (1981).

2.3. Helium chemistry

(He8) Radiative association of He and H^+

This rate of direct radiative association (He7) is quite small compared to inverse rotational predissociation, as shown by Flower & Roueff (1979), Roberge & Dalgarno (1982) and Kimura et al. (1993). The solid line in Fig. 2 shows our fit to the photorates computed by Roberge & Dalgarno (1982) (triangles). For comparison, the dashed line shows the rate of direct radiative association (Roberge & Dalgarno 1982).

(He11) Destruction of HeH^+ by H

The rate coefficient has been measured by Karpas et al. (1979) at $T = 300$ K (shown by a filled circle in Fig. 2). We have used a temperature-independent rate, which is equal to about one-half of the Langevin collision rate constant.

(He14) Photodissociation of HeH^+

This rate has been computed from detailed balance of the direct radiative association using a threshold energy of 1.96 eV and the rate coefficient of (He7). The result is shown by the solid line in Fig. 2. For comparison we also show the rate for reaction (He15) obtained by fitting (dashed line) the results of Roberge & Dalgarno (1982) (triangles).

2.4. Lithium chemistry

(Li3)-(Li4) Mutual neutralizations of Li and H

Following Stancil et al. (1996), we have adopted the same rate for (Li3) and (Li4). The solid line in Fig. 3 shows the rate obtained using the cross section of Peart & Hayton (1994). The long-dashed line is the rate determined by Janev & Radulović (1978). The dashed line is the rate adopted by Stancil et al. (1996).

(Li5) Radiative attachment of Li and e^-

We have used the cross section computed by Ramsbottom et al. (1994) for the inverse process (Li6) and detailed balance arguments to compute the rate shown in Fig. 3 by the solid line. The fit by Stancil et al. (1996), corrected as in Stancil & Dalgarno (1997), is shown by the dashed line.

(Li6) Photodetachment of Li^-

The solid line shows the rate obtained from the photodetachment cross section evaluated by Ramsbottom et al. (1994).

(Li9) Radiative association of LiH

This rate has been recently determined quantum-mechanically by Dalgarno et al. (1996) (squares) and Gianturco & Gori Giorgi (1996a) (triangles). Our fit to the results of Dalgarno et al. (1996) is shown by the solid line.

Table 2. Reaction rates for Deuterium species

	reaction	rate (cm^3 s^{-1} or s^{-1})	notes	reference
D1)	$\mathbf{D^+ + e \rightarrow D + \gamma}$		see text	
D2)	$\mathbf{D + \gamma \rightarrow D^+ + e}$		see text	
D3)	$\mathbf{D + H^+ \rightarrow D^+ + H}$	$3.7 \times 10^{-10} T_{\rm g}^{0.28} \exp\left(-\frac{43}{T_{\rm g}}\right)$	fit	WCD
D4)	$\mathbf{D^+ + H \rightarrow D + H^+}$	$3.7 \times 10^{-10} T_{\rm g}^{0.28}$	fit	WCD
D5)	$D + H \rightarrow HD + \gamma$	1.0×10^{-25}	estimate	LS
D6)	$D + H_2 \rightarrow H + HD$	$9.0 \times 10^{-11} \exp\left(-\frac{3876}{T_{\rm g}}\right)$	$T_{\rm g} > 250$, fit	ZM
D7)	$HD^+ + H \rightarrow H^+ + HD$		same as $H_2^+ + H$	KAH
D8)	$\mathbf{D^+ + H_2 \rightarrow H^+ + HD}$	2.1×10^{-9}		SAA
D9)	$HD + H \rightarrow H_2 + D$	$3.2 \times 10^{-11} \exp\left(-\frac{3624}{T_{\rm g}}\right)$	$T_{\rm g} > 200$	Sh
D10)	$\mathbf{HD + H^+ \rightarrow H_2 + D^+}$	$1.0 \times 10^{-9} \exp\left(-\frac{464}{T_{\rm g}}\right)$		SAA
D11)	$HD + H_3^+ \rightarrow H_2 + H_2D^+$	$(2.1 - 0.4 \log T_{\rm g}) \times 10^{-9}$	fit	ASa, MBH
D12)	$D + H^+ \rightarrow HD^+ + \gamma$		same as $H + H^+$	RP
D13)	$D^+ + H \rightarrow HD^+ + \gamma$		same as $H + H^+$	RP
D14)	$HD^+ + \gamma \rightarrow H + D^+$		same as $H_2^+ + \gamma$	
D15)	$HD^+ + \gamma \rightarrow H^+ + D$		same as $H_2^+ + \gamma$	
D16)	$HD^+ + e \rightarrow H + D$	$7.2 \times 10^{-8} T_{\rm g}^{-1/2}$	fit	St
D17)	$HD^+ + H_2 \rightarrow H_2D^+ + H$		same as $H_2^+ + H_2$	TH
D18)	$HD^+ + H_2 \rightarrow H_3^+ + D$		same as $H_2^+ + H_2$	TH
D19)	$D + H_3^+ \rightarrow H_2D^+ + H$	$2.0 \times 10^{-8} T_{\rm g}^{-1}$	uncertain	ASb
D20)	$H_2D^+ + e \rightarrow H + H + D$	$1.0 \times 10^{-6} T_{\rm g}^{-1/2} \times 0.73$		Da, La
D21)	$H_2D^+ + e \rightarrow H_2 + D$	$1.0 \times 10^{-6} T_{\rm g}^{-1/2} \times 0.07$		Da, La
D22)	$H_2D^+ + e \rightarrow HD + H$	$1.0 \times 10^{-6} T_{\rm g}^{-1/2} \times 0.20$		Da, La
D23)	$H_2D^+ + H_2 \rightarrow H_3^+ + HD$	$4.7 \times 10^{-9} \exp\left(-\frac{215}{T_{\rm g}}\right)$	$T_{\rm g} \leq 10^2$	
		5.5×10^{-10}	$T_{\rm g} > 10^2$	ASa, MBH, He
D24)	$H_2D^+ + H \rightarrow H_3^+ + D$	$2.0 \times 10^{-8} T_{\rm g}^{-1} \exp\left(-\frac{632}{T_{\rm g}}\right)$		ASb

ASa: Adams & Smith (1981); ASb: Adams & Smith (1985); Da: Datz et al. (1995); He: Herbst (1982); KAH: Karpas et al. (1979) La: Larsson et al. (1996); LS: Lepp & Shull (1984); MBH: Millar et al. (1989); RP: Ramaker & Peek (1976); SAA: Smith et al. (1982); Sh: Shavitt (1959); St: Strömholm et al. (1995); TH: Theard & Huntress (1974); WCD: Watson et al. (1978); ZM: Zhang & Miller (1989);

(Li10) Photodissociation of LiH

The solid line shows the analytical fit to the rate obtained by detailed balance of reaction (Li9).

(Li18) Radiative association of Li^+ and H

We have fitted (solid line) the results of Dalgarno et al. (1996) (squares). The values obtained by Gianturco & Gori Giorgi (1996a) are shown by triangles. The dashed line represents the analytic fit by Stancil et al. (1996).

(Li19) Radiative association of Li and H^+

As in the case of (Li18), we have adopted the results of Dalgarno et al. (1996) (triangles and solid line).

(Li25) Photodissociation of LiH^+

The dashed line shows the rate obtained by detailed balance applied to the radiative association reaction (Li18) adopting the rate by Dalgarno et al. (1996). Our fit is shown by the solid line.

3. Evolutionary models

We consider now the chemical and thermal evolution of the pregalactic gas in the framework of a Friedmann cosmological model. We start the calculations at $z = 10^4$ with all atomic species fully ionized and we follow their recombination down to to $z = 0$ assuming that no reionizing events have taken place in the Universe.

In order to calculate the abundances of the 21 elements included in the network, we have solved the set of coupled chemical rate equations of the form

$$\frac{{\rm d}n_i}{{\rm d}t} = k_{\rm form} n_j n_k - k_{\rm dest} n_i + \ldots, \quad (1)$$

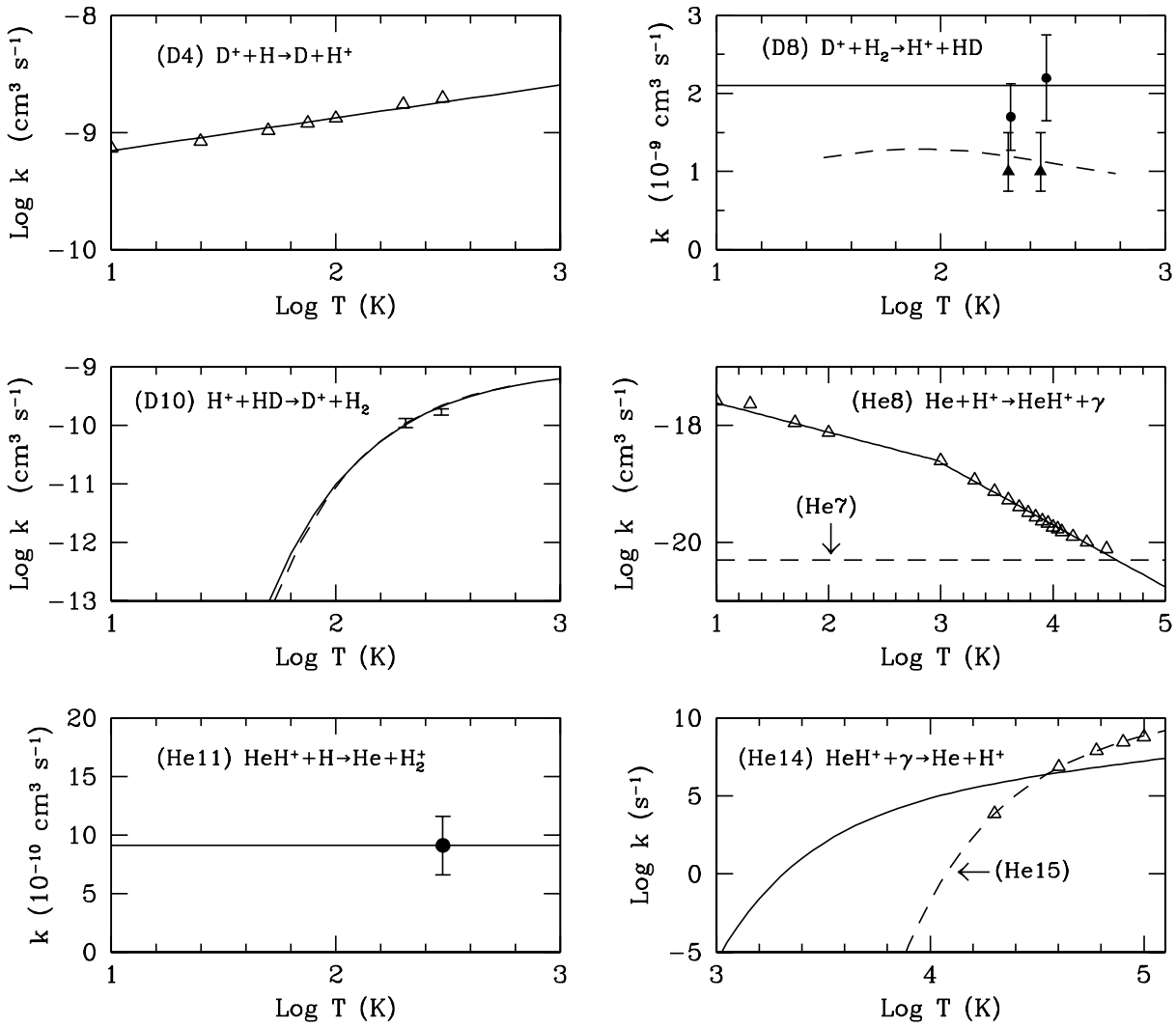

Fig. 2. Rate coefficients for HD and HeH^+ chemistry.

where $k_{\rm form}$ and $k_{\rm dest}$ are the formation and destruction reaction rates discussed in Sect. 2, and n_i is the number density of the reactant species i.

The temperature of the CBR is given by $T_{\rm r} = T_0(1+z)$ with $T_0 = 2.726$ K (Mather et al. 1994). The evolution of the gas temperature $T_{\rm g}$ is governed by the equation (see e.g. Puy et al. 1993; Palla et al. 1995)

$$\frac{{\rm d}T_{\rm g}}{{\rm d}t} = -2T_{\rm g}\frac{\dot{R}}{R} + \frac{2}{3kn}[(\Gamma-\Lambda)_{\rm Compton} + (\Gamma-\Lambda)_{\rm mol}]. \quad (2)$$

The first term represents the adiabatic cooling associated with the expansion of the Universe, R being the scale factor. The other two terms represent respectively the net transfer of energy from the CBR to the gas (per unit time and unit volume) via Compton scattering of CBR photons on electrons

$$(\Gamma-\Lambda)_{\rm Compton} = \frac{4k\sigma_{\rm T}aT_{\rm r}^4(T_{\rm r}-T_{\rm g})}{m_{\rm e}c}n_{\rm e}, \quad (3)$$

and via excitation and de-excitation of molecular transitions

$$(\Gamma-\Lambda)_{\rm mol} = \sum_k n_k \sum_{i>j}(x_i C_{ij} - x_j C_{ji})h\nu_{ij}, \quad (4)$$

where C_{ij} and C_{ji} are the collisional excitation and de-excitation coefficients and x_i are the fractional level populations. For the molecular heating and cooling of the gas we have considered the contribution of H_2, HD and LiH. A full discussion of the molecular parameters is given in the Appendix, where we present analytical fits and plots of the cooling functions in the temperature range $10\ {\rm K} \le T_{\rm g} \le 10^4$ K. Given the large range of validity, the cooling functions can be used in a variety of cosmological applications.

The energy transfer function $(\Gamma-\Lambda)_{\rm mol}$ can become an effective heating (cooling) source for the gas if the rate of collisional de-excitation of the roto-vibrational molecular levels is faster (slower) than their radiative decay (see Khersonskii 1986, Puy et al. 1993). In general, however, the contribution of molecules to the heating/cooling of the gas is very small.

Table 3. Reaction rates for Helium species

	reaction	rate (cm^3 s^{-1} or s^{-1})	notes	reference
He1)	$He^{++} + e \rightarrow He^+ + \gamma$	$1.891\times10^{-10}\left[\sqrt{\frac{T_g}{9.37}}\left(1+\sqrt{\frac{T_g}{9.37}}\right)^{0.2476}\times\left(1+\sqrt{\frac{T_g}{2.774\times10^6}}\right)^{1.7524}\right]^{-1}$		VF
He2)	$He^+ + \gamma \rightarrow He^{++} + e$	$5.0\times10^{1}T_r^{1.63}\exp\left(-\frac{590000}{T_r}\right)$	fit	Os
He3)	$He^+ + e \rightarrow He + \gamma$	$3.294\times10^{-11}\left[\sqrt{\frac{T_g}{15.54}}\left(1+\sqrt{\frac{T_g}{15.54}}\right)^{0.309}\times\left(1+\sqrt{\frac{T_g}{3.676\times10^7}}\right)^{1.691}\right]^{-1}$		VF
He4)	$He + \gamma \rightarrow He^+ + e$	$1.0\times10^{4}T_r^{1.23}\exp\left(-\frac{280000}{T_r}\right)$	fit	Os
He5)	$He + H^+ \rightarrow He^+ + H$	$4.0\times10^{-37}T_g^{4.74}$	$T_g \geq 8000$, fit	KLDD
He6)	$He^+ + H \rightarrow He + H^+$	$3.7\times10^{-25}T_g^{2.06}\times\left[1+9.9\exp\left(-\frac{T_g}{2570}\right)\right]$	fit by KF $T_g > 6000$	ZDKL
He7)	$He + H^+ \rightarrow HeH^+ + \gamma$	5.0×10^{-21}	rad. ass.	RD, KLDD
He8)	$\mathbf{He + H^+ \rightarrow HeH^+ + \gamma}$	$7.6\times10^{-18}T_g^{-0.5}$	$T_g \leq 10^3$,	
		$3.45\times10^{-16}T_g^{-1.06}$	$T_g > 10^3$ (inv. prediss.)	RD
He9)	$He + H_2^+ \rightarrow HeH^+ + H$	$3.0\times10^{-10}\exp\left(-\frac{6717}{T_g}\right)$		Bl
He10)	$He^+ + H \rightarrow HeH^+ + \gamma$	$1.6\times10^{-14}T_g^{-0.33}$	$T_g \leq 4000$, fit	
		1.0×10^{-15}	$T_g > 4000$, fit	ZD
He11)	$\mathbf{HeH^+ + H \rightarrow He + H_2^+}$	9.1×10^{-10}		KAH
He12)	$HeH^+ + e \rightarrow He + H$	$1.7\times10^{-7}T_g^{-0.5}$		YM
He13)	$HeH^+ + H_2 \rightarrow H_3^+ + He$	1.3×10^{-9}		Or
He14)	$\mathbf{HeH^+ + \gamma \rightarrow He + H^+}$	$6.8\times10^{-1}T_r^{1.5}\exp\left(-\frac{22750}{T_r}\right)$	fit	RD
He15)	$HeH^+ + \gamma \rightarrow He^+ + H$	$7.8\times10^{3}T_r^{1.2}\exp\left(-\frac{240000}{T_r}\right)$	fit	RD

Bl: Black (1978); KAH: Karpas et al. (1979); KLDD: Kimura et al. (1993); Or: Orient (1977); Os: Osterbrock (1989); RD: Roberge & Dalgarno (1982); VF: Verner & Ferland (1996); YM: Yousif & Mitchell (1989); ZD: Zygelman & Dalgarno (1990); ZDKL: Zygelman et al. (1989);

The chemical network is completed by the equation for the redshift

$$\frac{\mathrm{d}t}{\mathrm{d}z} = -\frac{1}{H_0(1+z)^2\sqrt{1+\Omega_0 z}}, \quad (5)$$

where $H_0 = 100\ h$ km s^{-1} Mpc^{-1} is the Hubble constant and Ω_0 the closure parameter.

The density $n(z)$ of baryons at redshift z is

$$n(z) = \Omega_\mathrm{b} n_\mathrm{cr}(1+z)^3, \quad (6)$$

where $n_\mathrm{cr} = 9.19\times10^{-6}h^2$ cm^{-3} is the critical density, and Ω_b is the ratio of the total to the critical density. This quantity is related to the baryon-to-photon ratio η by $\Omega_b = 3.66\times10^{-3}\eta_{10}h^{-2}$, with $\eta_{10} = 10^{10}\eta$.

4. Results

4.1. The standard model

Our standard model is characterized by a Hubble constant $h = 0.67$ (van den Bergh 1989), a closure parameter $\Omega_0 = 1$, and a baryon-to-photon ratio $\eta_{10} = 4.5$ (Galli et al. 1995). The initial fractional abundance of H, D, He and Li are taken from the standard big bang nucleosynthesis model of Smith et al. (1993).

The results are shown in Fig. 4, separately for each atomic element. The residual ionization fraction at $z = 1$ is $[\mathrm{e/H}] = 3.02\times10^{-4}$. Comparison with Model III of SLD which has the same values of the cosmological parameters (see Table 5) shows that the freeze-out ionization fraction is a factor of 2 smaller in our case, owing to the different treatment of H recombination.

The evolution of the abundance of H_2 follows the well known behaviour (e.g. Lepp & Shull 1983, Black 1991) where the initial steep rise is determined by the H_2^+ channel (reactions H9 and H10) followed by a small contribution from H^- at $z \simeq 100$ (reactions H3, H4 and H5). The freeze-out value of H_2 is $[H_2/H] = 1.1\times10^{-6}$, a value somewhat lower than found in similar studies, as a consequence of the net reduction of the ionization fraction.

Fig. 4 shows that all the ionic species reach very low fractional abundances. In particular, the steady drop of H^- at $z \lesssim 100$ is determined by mutual neutralization with H^+ (reac-

Table 4. Reaction rates for Lithium species

	reaction	rate (cm^3 s^{-1} or s^{-1})	notes	reference
Li1)	**Li$^+$ + e $\rightarrow$ Li + γ**	$1.036\times10^{-11}[\sqrt{T_\mathrm{g}/107.7}\times$ $(1+\sqrt{T_\mathrm{g}/107.7})^{0.612}\times$ $(1+\sqrt{T_\mathrm{g}/1.177\times10^7})^{1.388}]^{-1}$		VF
Li2)	**Li + γ $\rightarrow$ Li$^+$ + e**	$1.3\times10^3 T_\mathrm{r}^{1.45}\exp\left(-\frac{60500}{T_\mathrm{r}}\right)$	det. bal.	
Li3)	Li$^+$ + H$^-$ $\rightarrow$ Li + H	$6.3\times10^{-6}T_\mathrm{g}^{-0.5}-7.6\times10^{-9}+$ $2.6\times10^{-10}T_\mathrm{g}^{0.5}+2.7\times10^{-14}T_\mathrm{g}$	fit	PHa
Li4)	**Li$^-$ + H$^+$ $\rightarrow$ Li + H**		same as Li$^+$ + H$^-$	PHa
Li5)	**Li + e $\rightarrow$ Li$^-$ + γ**	$6.1\times10^{-17}T_\mathrm{g}^{0.58}\exp\left(-\frac{T_\mathrm{g}}{17200}\right)$	det. bal.	RBB
Li6)	**Li$^-$ + γ $\rightarrow$ Li + e**	$1.8\times10^2 T_\mathrm{r}^{1.4}\exp\left(-\frac{8100}{T_\mathrm{r}}\right)$	fit	RBB
Li7)	Li + H$^+$ $\rightarrow$ Li$^+$ + H	$2.5\times10^{-40}T_\mathrm{g}^{7.9}\exp\left(-\frac{T_\mathrm{g}}{1210}\right)$		KDS
Li8)	Li + H$^+$ $\rightarrow$ Li$^+$ + H + γ	$1.7\times10^{-13}T_\mathrm{g}^{-0.051}\exp\left(-\frac{T_\mathrm{g}}{282000}\right)$		SZ
Li9)	**Li**(^2S) **+ H $\rightarrow$ LiH +** γ	$(5.6\times10^{19}T_\mathrm{g}^{-0.15}+7.2\times10^{15}T_\mathrm{g}^{1.21})^{-1}$		DKS, GGGa
Li10)	**LiH + γ $\rightarrow$ Li**(^2S) **+ H**	$8.3\times10^4 T_\mathrm{r}^{0.3}\exp\left(-\frac{29000}{T_\mathrm{r}}\right)$	det. bal.	
Li11)	Li(^2P) + H $\rightarrow$ LiH + γ	$2.0\times10^{-16}T_\mathrm{g}^{0.18}\exp\left(-\frac{T_\mathrm{g}}{5100}\right)$	$A^1\Sigma^+\rightarrow X^1\Sigma^+$	GGGb
Li12)	Li(^2P) + H $\rightarrow$ LiH + γ	$1.9\times10^{-14}T_\mathrm{g}^{-0.34}$	$B^1\Pi\rightarrow X^1\Sigma^+$	GGGb
Li13)	Li + H$^-$ $\rightarrow$ LiH + e	4.0×10^{-10}	estimate	SLD
Li14)	**Li$^-$ + H $\rightarrow$ LiH + e**	4.0×10^{-10}	estimate	SLD
Li15)	LiH$^+$ + H $\rightarrow$ LiH + H$^+$	$1.0\times10^{-11}\exp\left(-\frac{67900}{T_\mathrm{g}}\right)$	estimate	SLD
Li16)	LiH + H$^+$ $\rightarrow$ LiH$^+$ + H	1.0×10^{-9}	estimate	SLD
Li17)	**LiH + H $\rightarrow$ Li + H$_2$**	2.0×10^{-11}	estimate	SLD
Li18)	**Li$^+$ + H $\rightarrow$ LiH$^+$ +** γ	$\mathrm{dex}[-22.4+0.999\log T_\mathrm{g}-0.351(\log T_\mathrm{g})^2]$		DKS, GGGa
Li19)	**Li + H$^+$ $\rightarrow$ LiH$^+$ +** γ	$4.8\times10^{-14}T_\mathrm{g}^{-0.49}$		DKS
Li20)	LiH + H$^+$ $\rightarrow$ LiH$^+$ + H	1.0×10^{-9}	estimate	SLD
Li21)	LiH + H$^+$ $\rightarrow$ Li$^+$ + H$_2$	1.0×10^{-9}	estimate	SLD
Li22)	**LiH$^+$ + e $\rightarrow$ Li + H**	$3.8\times10^{-7}T_\mathrm{g}^{-0.47}$	estimate	SLD
Li23)	LiH$^+$ + H $\rightarrow$ Li + H$_2^+$	$9.0\times10^{-10}\exp\left(-\frac{66400}{T_\mathrm{g}}\right)$	estimate	SLD
Li24)	**LiH$^+$ + H $\rightarrow$ Li$^+$ + H$_2$**	3.0×10^{-10}	estimate	SLD
Li25)	**LiH$^+$ +** γ **$\rightarrow$ Li$^+$ + H**	$7.0\times10^2\exp\left(-\frac{1900}{T_\mathrm{r}}\right)$	det. bal.	DKS, GGGa
Li26)	LiH$^+$ + γ $\rightarrow$ Li + H$^+$	$3.35\times10^7 T_\mathrm{r}\exp\left(-\frac{97000}{T_\mathrm{r}}\right)$	det. bal.	SLD

DKS: Dalgarno et al. (1996); GGGa: Gianturco & Gori Giorgi (1996a); GGGb: Gianturco & Gori Giorgi (1996b); KDS: Kimura et al. (1994); PHa: Peart & Hayton (1994); RBB: Ramsbottom et al. (1994); SLD: Stancil et al. (1996); SZ: Stancil & Zygelman (1996); VF: Verner & Ferland (1996)

Table 5. Ionization fraction at $z = 10$

H_0	Ω_0	Ω_b	T_0 (K)	[e/H] (this work)	[e/H] (other)
67	1	0.0367	2.726	3.3(-4)	6.5(-4) [SLD-III]
50	0.1	0.1	2.7	5.1(-5)	5.0(-5) [B]
50	1	0.1	2.726	1.7(-4)	3.2(-4) [SLD-I]
100	1	0.1	2.7	8.3(-5)	7.8(-5) [LB]

B: Black (1991); LB: Latter & Black (1991); SLD-I, SLD-III: Models I and III of Stancil et al. (1996)

tion H7). As discussed before, the rate for this reaction is still uncertain, but the net effect on the final abundance of H_2 is quite small. The reason is that the rates differ only at low temperatures (below $\sim$ 100 K) when the H_2 formation via the H^- channel is already completed. In fact, adopting the Dalgarno & Lepp (1987) rate for reaction (H7) leads to a 10% difference in the H_2 abundance. On the contrary, the abundance of H^- is quite affected by the choice of the rate of (H7): our final H^- abundance at $z = 1$ is three times smaller than that obtained using Dalgarno & Lepp (1987).

The formation of H_2^+ is controlled by radiative association (H8) and photodissociation (H9) at $z \geq 100$, whereas at lower redshifts there is a contribution from HeH^+ (reaction He11) that explains the gentle rise up to $[H_2^+/H_2] \simeq 10^{-6}$. An additional channel for H_2^+ formation is the associative ionization reaction $H + H(n = 2) \rightarrow H_2^+ + e$ (Rawlings et al. 1993; see also Latter & Black 1991 for H_2 formation). The rate coefficient for this process is $\sim$ 4 orders of magnitude faster than (H8)

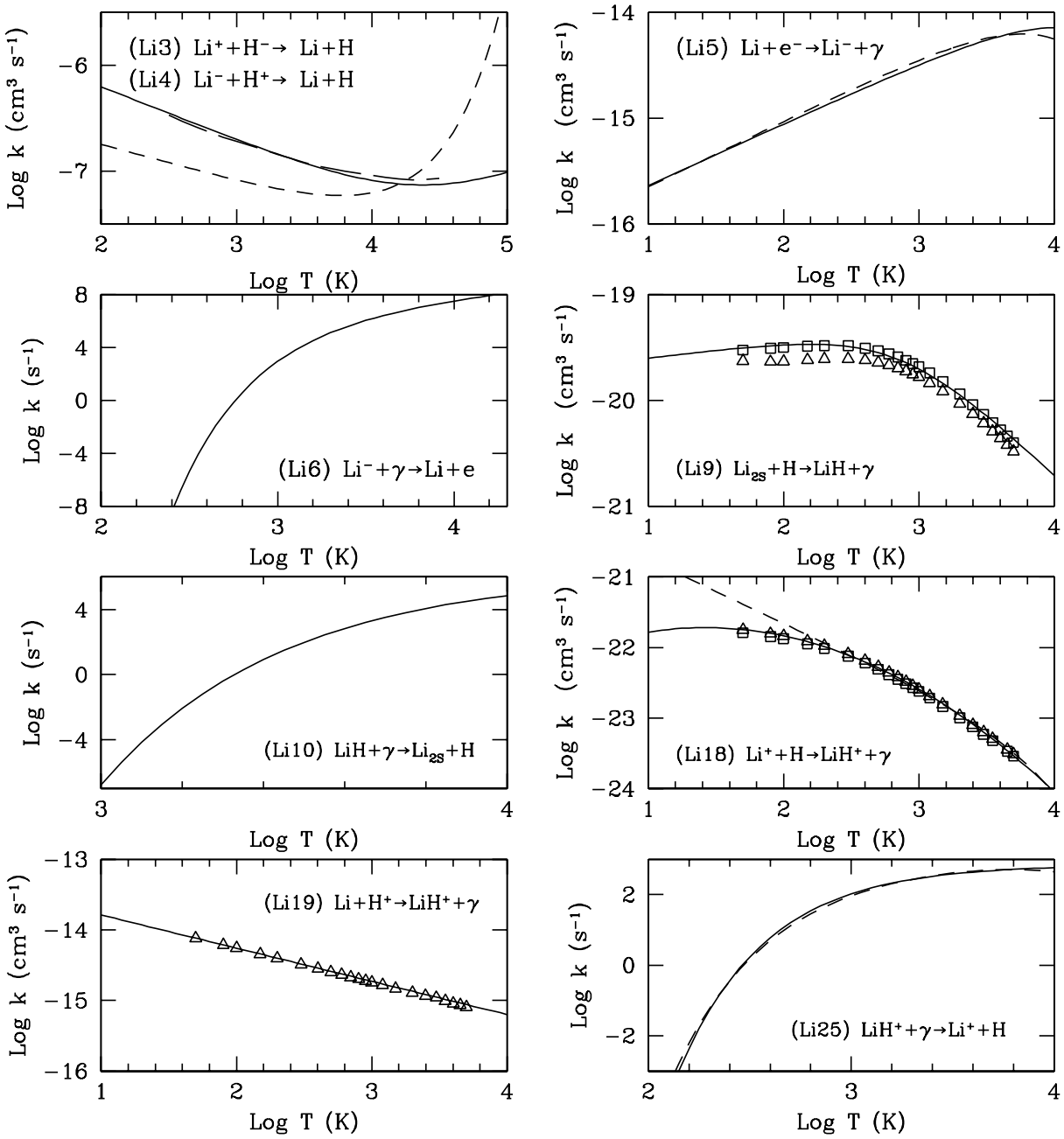

Fig. 3. Rate coefficients for LiH chemistry.

but the extremely low fractional population of the $n = 2$ level of H ($\ll 10^{-13}$) makes associative ionization not competitive with radiative association. The evolution of H_2^+ and, to a large extent, the abundance of H_2 depend crucially on the adopted photodissociation rate. This is clearly shown in Fig. 5 where the results obtained with various choices of the rate discussed in Sect. 2.1 are compared with the results of the standard model (shown by the solid line). Photodissociation of H_2^+ from $v = 0$ (dashed line) would result in an enhancement of a factor ~ 200 of the final H_2 abundance, whereas photodissociation from $v = 9$ (long-dashed line), would delay the redshift of formation of H_2^+ from $z \simeq 10^3$ to $z \simeq 300$ and of H_2 from $z \simeq 600$ to $z \simeq 250$. However, the asymptotic abundances of both species are left unchanged.

We believe that the uncertainty in the redshift evolution of H_2 is not as large as that shown in Fig. 5, because photodissociation from $v = 0$ is extremely unlikely to occur at $z \simeq 10^3$. The actual behaviour of the H_2 abundance should be intermediate between the two curves in Fig. 5 corresponding to photodissociation from $v = 9$ and LTE. The conditions for a distribution of level populations in LTE may be marginally satisfied, considering the fact that the radiative decay rates (Posen et al. 1983) are much faster than the collisional excitation rates at the typical densities, but we know from the work of Ramaker & Peek

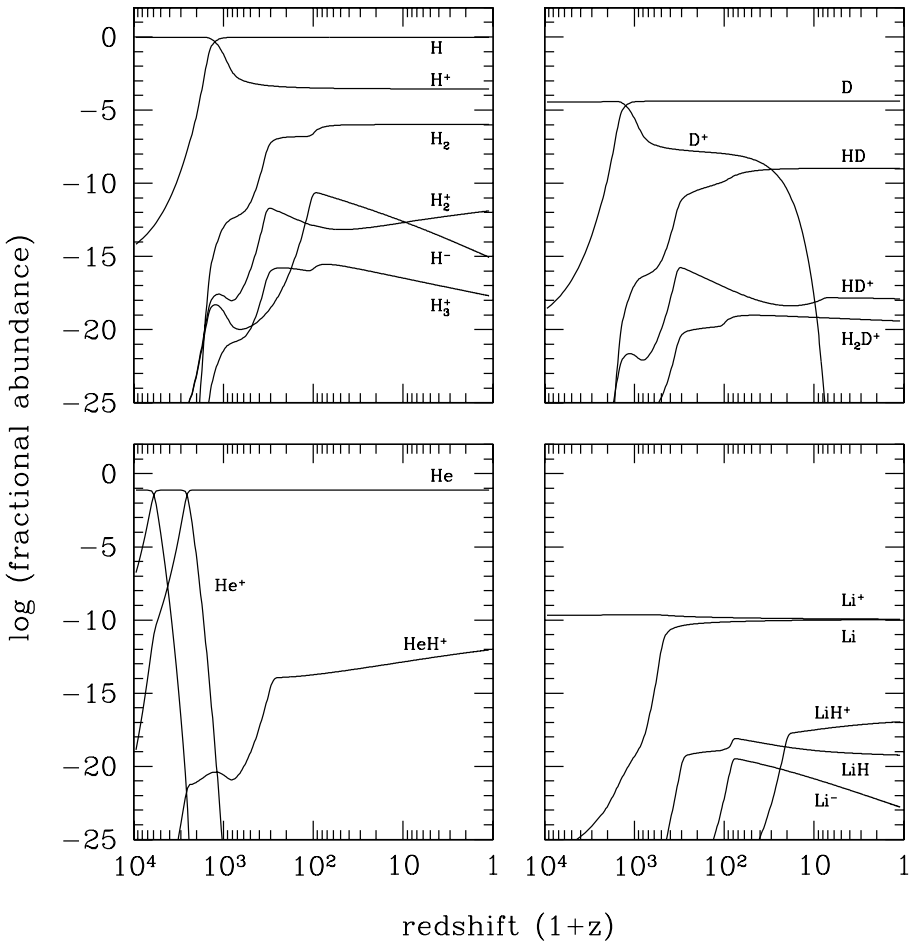

Fig. 4. The evolution of all the chemical species considered in the standard model as a function of redshift. The four panels show the results for H (upper left), D (upper right), He (lower left), and Li (lower right).

(1976) that the reverse reaction (H8) forms H_2^+ preferentially in excited states. In such a case, photodissociation would take place from high vibrational levels and the LTE rate may underestimate somehow the actual rate. Thus, we conclude that the uncertainty is limited to the redshift of formation of H_2 molecules and not to their final abundance.

As for deuterium, Fig. 4 shows that the evolution of D^+ is very sensitive to the charge exchange reactions (D3)–(D4). At $z < 40$, the abundance of D^+ drops precipitously due to the exponential factor in the reaction rate (D3). The only molecule formed in significant amount is HD, whose evolution with redshift follows closely that of H_2. However, its abundance at freeze-out is $[HD/H_2] \simeq 10^{-3}$. More important, the asymptotic value of $[HD/H_2]$ becomes about 10^{-3} with an enhancement factor of $\sim$30 from the initial [D/H] abundance. This is due to the large fractionation implied by reaction (D8). The behaviour of HD^+ follows that of H_2^+ up to $z \simeq 100$, while at lower redshifts its evolution is dominated by reaction (D12). The flattening at $z < 10$ reflects the behaviour of the reaction rate at temperatures below ~ 20 K.

The case of $H_2D^+$is of interest after the suggestion by Dubrovich (1993) and Dubrovich & Lipovka (1995) that in the early universe this molecule could reach significant abundances (up to $[H_2D^+/H_2] = 10^{-5}$) and that spectral features associated with the rovibrational transitions might be detectable in the spectrum of the CBR. Such a high abundance would result from the complete conversion of H_3^+ into H_2D^+ because of deuterium fractionation at low temperatures ($T < 50$ K). However, it is very unlikely that this mechanism could work in the conditions of the primordial gas, since the abundance of H_3^+ ions is quite low due to the absence of ionizing sources (see Fig. 4). In present-day molecular clouds, searches for the rotational transitions of H_2D^+ have yielded a fractional abundance of 3×10^{-11} (Boreiko & Betz 1993). The results shown in Fig. 4 indicate that the final abundance of $H_2D^+$is extremely small $[H_2D^+/H] \simeq 5 \times 10^{-14}$, and $[H_2D^+/H_3^+] \simeq 10^{-2}$. It is clear from our models that the presence of H_2D^+ molecules can hardly affect the shape of the CBR (in order to see detectable effects on the CBR, Dubrovich & Lipovka (1993) assume an abundance of 10^{-8}). On the other hand, the isotopic ratio is greatly enhanced with respect to the primordial abundance $[D/H] = 4 \times 10^{-5}$, due to fractionation effects.

According to the results shown in Fig. 4, the main molecular species containing helium is HeH^+, formed by the radiative association of He and H^+. As emphasized by Lepp & Shull (1984), this reaction is slower than the usual formation mode via association of He^+ and H, but since the abundance of He^+ is quite small, reaction (He8) takes over. The HeH^+ ions are removed by CBR photons and at $z \lesssim 250$ also by collisions with H atoms to reform H_2^+ (reaction He11). This explains the

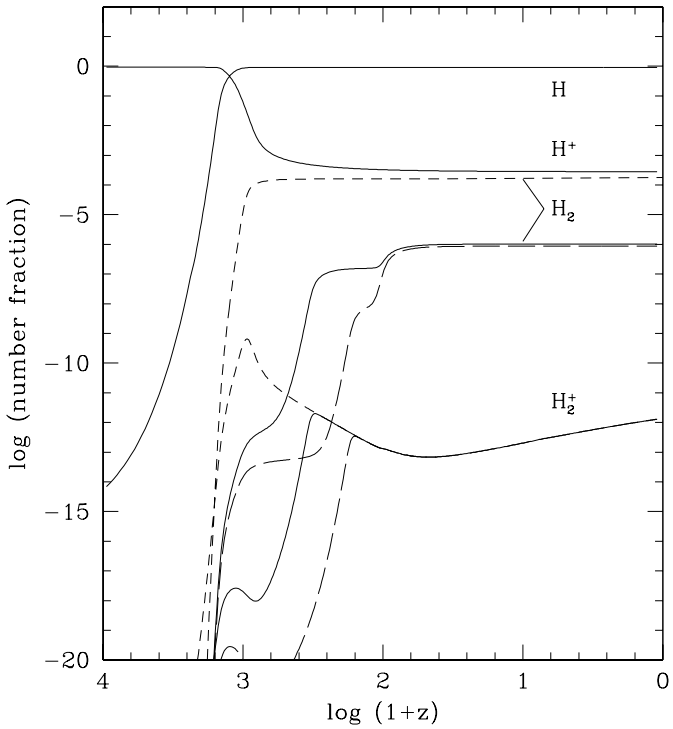

Fig. 5. Effects of varying the photodissociation rate of H_2^+ on the evolution of H_2 and H_2^+. The solid curves are for the standard models, whereas the results obtained with photodissociation from the $v = 0$ and $v = 9$ vibrational levels of H_2^+ are shown by the *dashed* and *long dashed* lines, respectively.

abrupt change in the slope of the curve of HeH^+ shown in Fig. 4. The final abundance is small, $[HeH^+/H] \sim 6 \times 10^{-13}$ at $z = 1$.

Finally, the chemistry of lithium is complicated, but the molecular abundances are indeed very small. The more abundant complex is LiH^+ whose formation is controlled by the radiative association of Li^+ and H (see Dalgarno & Lepp 1987). As shown in Fig. 4, lithium remains more ionized at low redshifts and this explains why LiH is less abundant than LiH^+. The final abundance of LiH^+ is $\simeq 10^{-17}$ at $z = 1$.

4.2. Dependence on the cosmological parameters

The final values of the molecular abundances depend on the choice of the cosmological parameters. Each model is in fact specified by three parameters η_{10}, Ω_0 and h. The observational (and theoretical) uncertainties associated with each of them are still rather large. We have selected as standard model that that better fits the constraints imposed by the observations of the abundances of the light elements. To gauge the effects that a change of η_{10} induces on the chemistry network, we have run a model with η_{10}=8.0, the maximum value still compatible with the constraints on standard big bang nucleosynthesis given by observations of lithium in Pop-II stars (Bonifacio & Molaro 1997). The results are given in Table 6 for a direct comparison with the standard case. Note that the abundance of H_2 is the same in the two models, making this molecule a poor diagnostic of cosmological models. Lithium molecules are quite sensitive to η_{10}, showing an increase of a factor of 3–4. For the other species, however, a higher value of η_{10} implies a lower final abundance as a result of the lower initial value of each element predicted by the standard big bang nucleosynthesis which compensates for the higher total baryon density. As shown by Palla et al. (1995), larger variations of the molecular abundances than those shown in Table 6 can be expected for more drastic variations of the other cosmological parameters: both LiH and HD can vary by 2 or 3 orders of magnitudes by allowing changes to Ω_0 and h of a factor of 5 and 2, respectively. However, current observations indicate that a high value of the Hubble constant is unlikely, and that a universe with $\Omega_0 < 1$, as in the case of a nonzero value of the cosmological constant, is less favored by theoretical models.

5. The minimal model

The chemical network discussed in Sect. 2 consists of 87 reactions, 69 collisional and 18 radiative. Although the integration of such system does not present particular difficulties (apart for the intrinsic stiffness of the rate equations) or require exceedingly long computer times, for a better understanding of the chemistry of the primordial gas it is more convenient to reduce the reactions to only those that are essential to accurately model the formation/destruction of each molecular species. Such a reduced system has been called the *minimal model*. Abel et al. (1997) have devised a reduced network in their discussion of the non-equilibrium effects and chemical dynamics of the primordial gas. However, their application differs from ours, since they are mainly interested in the formation of H_2 in the post-shock layer of a cosmological pancake and consider only collisional processes.

Our minimum model consists of the 33 reactions indicated in the diagram shown in Fig. 6. The main reactions are listed in bold face in Tables 1 to 4. Notice that in order to describe fully the H_2 chemistry only 11 reactions out of 22 are needed. The formation of H_2 involves two reaction sequences with H^- and H_2^+ ions whose abundance is restricted by photodestruction processes. However, for H^- a competing destruction channel is the mutual neutralization with H^+ ions which contributes $\sim$ 20–40% to the total rate at redshifts $z \lesssim 100$. The H_2 system would be closed if not for the external source of H_2^+ ions coming from the destruction of HeH^+ by H atoms (reaction He11) at redshifts $z \lesssim 250$. It is important to consider this path since it modifies substantially the evolution of H_2^+ (see Fig. 4), although it does not affect the final abundance of H_2 molecules. As we have already noted, in the absence of this channel the final abundance of H_2^+ would be of the same order as that of H_3^+, because of the importance of reaction (H19).

The chemistry of deuterium is rather simple and only 6 reactions out of 24 need to be considered. The molecule HD is formed rapidly by reaction (D8) which involves ionized deuterium. Thus, it is important to consider all the reactions that determine the ionization balance. The main destruction route is by reaction (D10), while other reactions involving H_3^+ (D11) and H (D9) are much less important.

Table 6. Sensitivity of abundances to η_{10}

			$z = 2000$				$z = 1$					
η_{10}	X	Y	H	He	D	Li	[e/H]	[H_2/H]	[HD/H]	[HeH^+/H]	[LiH^+/H]	[LiH/H]
4.5	0.757	0.243	0.926	7.4(-2)	4.0(-5)	2.2(-10)	3.0(-4)	1.1(-6)	1.2(-9)	6.2(-13)	9.4(-18)	7.1(-20)
8.0	0.751	0.249	0.923	7.6(-2)	1.7(-5)	7.0(-10)	1.7(-4)	1.1(-6)	5.0(-10)	4.3(-13)	2.5(-17)	2.3(-19)

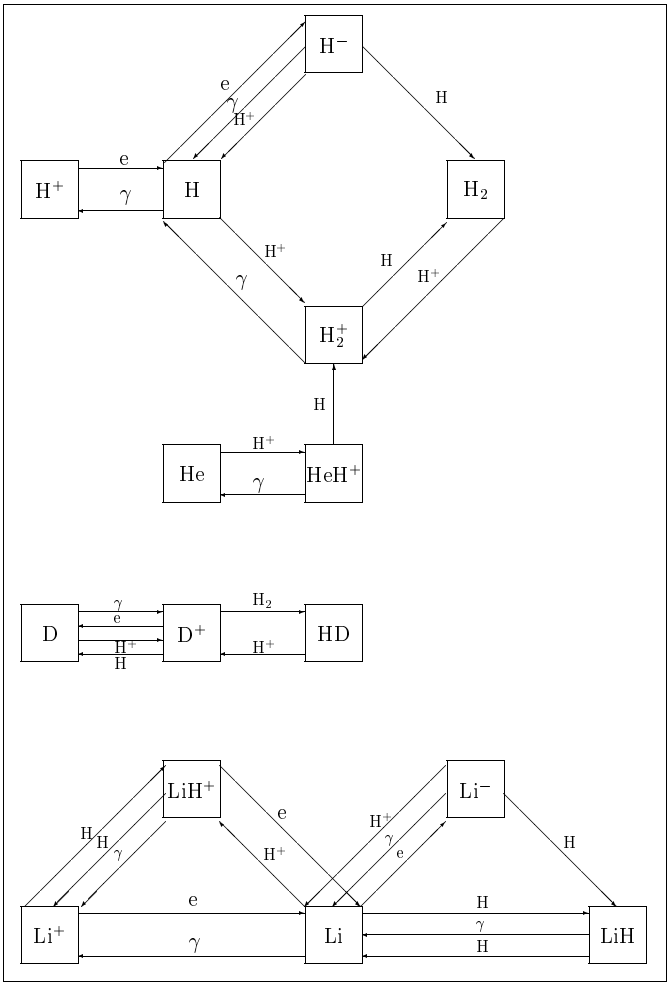

Fig. 6. The minimal model for the main chemical species

Finally, the chemistry of Li is more complex than the rest and even the reduced network contains a large number of reactions (14 out of 26). This is mainly due to the fact that lithium remains partly ionized and the routes to the formation of LiH and LiH^+ compete effectively with each other. Note also that at redshifts $z \lesssim 100$, the main route to LiH formation is from associative detachment of Li^- ions with H. This process gradually removes Li^- and the abundance of LiH reaches a constant value.

6. Comparison with previous work

In order to make accurate comparisons with the results obtained in previous studies, we have run models with the same reaction rates adopted in our standard case, but differing cosmological parameters to reproduce exactly the choices of the various authors listed in Table 7.

Table 7. Values of the cosmological parameters

Model	h	Ω_0	Ω_b	T_0 (K)
PGS	67	1	0.0367	2.726
LS	50	0.1	0.1	3
PALLP	50	1	0.1	2.7
B	50	0.1	0.1	2.7
GS	75	1	0.02	2.7

PGS: Palla et al. (1995); LS: Lepp & Shull (1983); PALLP: Puy et al. (1993); B: Black (1991); GS: Giroux & Shapiro (1996)

The results are shown in Fig. 7, where we compare the predictions of our model (solid lines) with those of Palla et al. (1995) (upper left panel), Lepp & Shull (1984) (upper right panel), Puy et al. (1993) (lower left panel), and Black (1991) (lower right panel), all indicated by dashed lines. A common feature in the first three cases is a dramatic reduction of the abundance of LiH by 7–9 orders of magnitude, due to the replacement of the semiclassical estimate of the rate of radiative association (Lepp & Shull 1984) with the quantal calculations by Dalgarno et al. (1996) and Gianturco & Gori Giorgi (1996a).

With respect to our earlier study of primordial chemistry, the more accurate treatment of H recombination results in a decreased residual electron fraction by a factor 2–3 (see also Table 5). This, in turn, has a direct impact on the H_2 and HD abundances, which are lower by a factor ~ 5. Otherwise, the evolution with redshift of these two species follows the same behaviour.

Similar considerations apply to the comparison with the results obtained earlier by Lepp & Shull (1984) for H, H^+ and H_2. However, it is worth noticing that in their model the formation of HD occurs through the analogues of the H^- and H_2^+ channels, at rates diminished by the cosmological D/H ratio, plus a negligible contribution from direct radiative association of H and D. In contrast, we have found that the main reaction responsible for the formation of HD is the isotope exchange reaction (D8) which has no counterpart in the hydrogen chemical network. Therefore, despite their higher residual electron fraction, their asymptotic abundance of HD is underestimated by about one order of magnitude.

Puy et al. (1993) obtained abundances of H_2 and HD about one order of magnitude larger than ours, owing to their unrealistic choice of the photodissociation rate (H9) by von Bush &

Dunn (1968), valid for a LTE distribution of level populations at $T = 100$ C. The higher abundance of H_2^+ results in a higher abundance of H_2 formed through this channel, and, in turn, to a correspondingly larger abundance of HD through reaction (D8).

Finally, the results of Black (1991), Latter & Black (1991), and Giroux & Shapiro (1996) allow a direct comparison of the evolution of some less abundant species like H^-, H_2^+ and HeH^+. The agreement with our results and those by Black (1991) is extremely good: the abundance of H, H^+ and H_2 agree within less than a factor 1.5 from $z = 10^3$ to $z = 10$, while the abundances of H^-, H_2^+, although differing by a factor ~ 3, follow remarkably the same behaviour with redshift. Only HeH^+ shows a marked (but unconsequential) difference for $z > 300$, probably due to a different choice of the photodissociation rate (He14). On the other hand, the comparison with Giroux & Shapiro (1996) shows a different behaviour of H_2^+ at $z \lesssim 100$ resulting from the neglect of the HeH^+ channel for H_2^+ formation.

7. Conclusions

The main results of the present study can be summarised as follows:

1) We have followed the chemical evolution of the primordial gas after recombination by computing the abundances of 21 species, 12 atomic and 9 molecular, by using a complete set of reaction rates for collisional and radiative processes. The rates which are critical for a correct estimate of the final molecular abundances have been analysed and compared in detail.

2) One of the major improvements of this work is the use of a better treatment of H recombination that leads to a reduction of a factor 2–3 in the abundance of electrons and H^+ at freeze-out, with respect to previous studies. The lower residual ionization has a negative effect on the chemistry of the primordial gas in which electrons and protons act as catalysts in the formation of the first molecules.

3) In the standard model ($h = 0.67$, $\eta_{10} = 4.5$, $\Omega_0 = 1$ and $[\mathrm{D/H}] = 4.3 \times 10^{-5}$), the residual fractional ionization at $z = 1$ is $[\mathrm{e/H}] = 3.02 \times 10^{-4}$, and the main molecular species have fractional abundances $[\mathrm{H_2/H}] = 1.1 \times 10^{-6}$, $[\mathrm{HD/H_2}] = 1.1 \times 10^{-3}$, $[\mathrm{HeH^+/H}] = 6.2 \times 10^{-13}$, $[\mathrm{LiH^+/H}] = 9.4 \times 10^{-18}$ and $[\mathrm{LiH/LiH^+}] = 7.6 \times 10^{-3}$.

4) As for molecular hydrogen, its final abundance does not depend on the model parameters, making this molecule a poor diagnostic of cosmological scenarios. The largest uncertainty resides in the accurate knowlwedge of the photodissociation rate of H_2^+. A detailed treatment of the reaction kinetics of this reaction would be required.

5) We have presented a minimal model consisting of 11 reactions for H_2, 6 for HD, 3 for HeH^+ and 14 for LiH which reproduces with excellent accuracy the results of the full chemical network, regardless of the choice of the cosmological parameters.

6) Finally, we have computed accurate expressions for the cooling functions of H_2, HD and LiH in a wide range of density and temperature that can be conveniently used in a variety of comological applications.

Acknowledgements. It is a pleasure to thank T. Abel, A. Dalgarno, D. Flower and P. Stancil for very useful conversations on various aspects of the chemistry of the early universe.

Appendix A: excitation coefficients and cooling

We have evaluated the contribution of H_2, HD, and LiH to the heating/cooling properties of the primordial gas. For each molecule, the steady-state level populations are obtained at any z by solving the balance equations

$$x_{j'} \sum_{j'} (R_{jj'} + C_{jj'}) = \sum_{j'} x_{j'} (R_{j'j} + C_{j'j}), \tag{A1}$$

where j and j' indicate a generic couple of rovibrational levels. The collisional transition probabilities $C_{jj'}$ and $C_{j'j}$ are obtained by multiplying the corresponding excitation coefficients $\gamma_{jj'}$ and $\gamma_{j'j}$ by the gas density. The terms $R_{jj'}$ and $R_{j'j}$ are the radiative excitation and de-excitation rates, that can be expressed in terms of the Einstein coefficients $A_{jj'}$ and $B_{jj'}$,

$$R_{jj'} = \begin{cases} A_{jj'} + B_{jj'} u(\nu_{jj'}, T_\mathrm{r}), & j' < j, \\ B_{jj'} u(\nu_{jj'}, T_\mathrm{r}), & j' > j, \end{cases} \tag{A2}$$

where $u(\nu_{jj'}, T_\mathrm{r})$ is the energy density of the radiation per unit frequency at the temperature T_r,

$$u(\nu_{jj'}, T_\mathrm{r}) = \frac{8\pi h \nu_{jj'}^3}{c^2} \left[\exp(h\nu_{jj'}/kT_\mathrm{r}) - 1\right]^{-1}. \tag{A3}$$

To evaluate the cooling function $\Lambda_\mathrm{mol}(z)$, the radiative and collisional transition probabilities and the frequencies of the roto-vibrational transitions must be specified for each molecule. These data can be easily found in the literature only for H_2, that is obviously the best studied case, but are quite sparse for the two other species we have considered. As for LiH, the relevant quantities have been collected and critically examined by Bougleux & Galli (1997), and we refer the interested reader to their paper (in particular, see their Appendix B). Here, we limit ourselves to a discussion of the adopted coefficients for HD and H_2.

A.1. H_2

Ortho- and para-H_2 were assumed to be in their equilibrium $(3 : 1)$ ratio. The radiative rates were calculated by Turner et al. (1977). Since in some cases where H_2 plays a major role the gas temperature can reach more than one thousand degrees, it is not sufficient to consider only the ground ($v = 0$) vibrational state. The choice of the rovibrational H-H_2 collisional coefficients is very delicate, since the published data may vary up to factors of 50–100 according to different authors (see e.g. Shull & Beckwith 1982, Mandy & Martin 1993, Sun & Dalgarno 1994, Flower 1997a,b), and the resulting H-H_2 cooling functions may differ by considerable amounts. For cosmological problems, one generally adopts the analytical expressions given by Hollenbach & McKee (1979, 1989) or Lepp & Shull (1983). These formulae appear now to suffer considerably from the limitations and uncertainties associated with the collisional coefficients available

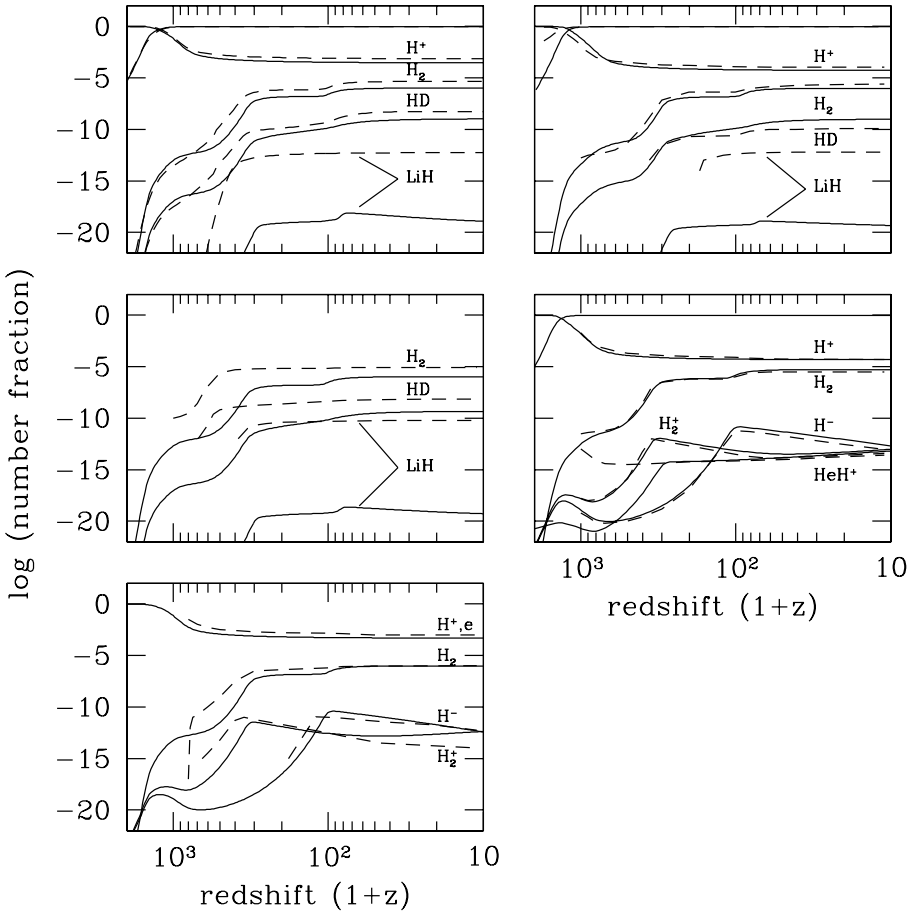

Fig. 7. Comparison between the results of the standard model (solid lines) and those of Palla et al. (1995) (*upper left*), Lepp & Shull (1984) (*upper right*), Puy et al. (1993) (*middle left*), Black (1991) (*middle right*), and Giroux & Shapiro (1996) (*lower left*), all indicated by dashed lines.

at the time. At low temperatures, the uncertainty is associated with the choice of the interaction potential, since it is very difficult, even nowadays, to calculate the potential in the interaction region to the requisite level of accuracy ($\sim 10^{-3}$ hartrees). The recently developed potentials LSTH (Truhlar & Horowitz 1978), DMBE (Varandas et al. 1987), BKMP1 (Boothroyd et al. 1991), BKMP2 (Boothroyd et al. 1996) and PBSL (Partridge et al. 1993) have been adopted by various groups to generate sets of collisional cross sections and rate coefficients, using different methods. Table A1 shows a comparison of the resulting values of γ_{20} at $T_{\rm g} = 10^3$ K.

At temperatures higher than ~ 600 K, we have adopted the set of rovibrational H-H_2 rate coefficients computed by Mandy & Martin (1993). The corresponding cooling function has been determined by Martin et al. (1996). At lower temperatures, we have adopted the collisional coefficients recently computed by Forrey et al. (1997) that match those of Mandy & Martin (1993) at $T = 10^3$ K. We have fitted the tabulated results by expressions like

$$\gamma_{J,J'} = a_0 + a_1 T_{\rm g} + a_2 T_{\rm g}^2 + a_3 T_{\rm g}^3, \tag{A4}$$

where $\gamma_{J,J'}$ is in cm^3 s^{-1}, and the coefficients a_i are listed in Table A2. Different choices (like, e. g. Flower 1997a,b) are of course possible, and produce differences of a factor ~ 2 in the cooling function.

Table A1. H-H_2 Collisional Deexcitation: Comparison of Different Results at $T_{\rm g} = 10^3$ K

Potential	Method	γ_{20} (cm^3 s^{-1})	Reference
LSTH	rigid rotor	7.0×10^{-13}	GT
LSTH	quasi-classical	3.1×10^{-12}	MM
LSTH	quasi-classical	3.0×10^{-12}	LBD
DMBE	quasi-classical	2.8×10^{-11}	LBD
DMBE	quantal	2.4×10^{-11}	SD
BKMP1	quantal	1.3×10^{-12}	Fa
PBSL	quantal	8.7×10^{-13}	Fb
BKMP2	quantal	2.9×10^{-12}	FBDL

GT: Green & Thrular (1979); MM: Mandy & Martin (1993); LBD: Lepp et al. (1995); SD: Sun & Dalgarno (1994); Fa: Flower (1997a); Fb: Flower (1997b); FBDL: Forrey et al. (1997)

It is convenient to express the H_2 cooling function $\Lambda_{\rm H_2}$ (in erg cm^3 s^{-1}) in the form given by Hollenbach & McKee (1979),

$$\Lambda_{\rm H_2}[n({\rm H}), T_{\rm g}] = \frac{\Lambda({\rm LTE})}{1 + [n^{\rm cr}/n({\rm H})]}, \tag{A5}$$

Table A2. H-H_2 Collisional De-excitation Coefficients (from Forrey et al. 1997)

J'	J	a_0	a_1	a_2	a_3
2	0	2.93(-14)	1.21(-15)	2.16(-19)	1.32(-21)
3	1	8.34(-14)	5.97(-16)	7.76(-19)	1.72(-21)
4	2	7.54(-14)	2.65(-16)	2.14(-19)	2.65(-21)
5	3	2.95(-14)	1.21(-16)	5.53(-19)	2.51(-21)

where $\Lambda_{\rm H_2}({\rm LTE})$ is the LTE cooling function given by Hollenbach & McKee (1979), $n^{\rm cr}$ is the critical density defined as

$$\frac{n^{\rm cr}}{n({\rm H})} = \frac{\Lambda_{\rm H_2}({\rm LTE})}{\Lambda_{\rm H_2}[n({\rm H}) \rightarrow 0]}, \tag{A6}$$

and $\Lambda[n({\rm H}) \rightarrow 0]$ is the low-density limit of the cooling function, independent of the H density. The latter can be computed from the collisional and radiative deexcitation coefficients described above, and the result is well approximated by the expression

$$\begin{aligned}\log \Lambda_{\rm H_2}[n({\rm H}) \rightarrow 0] \\ = -103.0 + 97.59 \log T_{\rm g} - 48.05 (\log T_{\rm g})^2 \\ +10.80 (\log T_{\rm g})^3 - 0.9032 (\log T_{\rm g})^4,\end{aligned} \tag{A7}$$

over the range $10 \ {\rm K} \leq T_{\rm g} \leq 10^4 \ {\rm K}$.

The H-H_2 cooling function is shown in Fig. A1 for two values of the H density, $n({\rm H}) = 0.1 \ {\rm cm}^{-3}$ and $n({\rm H}) = 10^6 \ {\rm cm}^{-3}$. The cooling functions given by Hollenbach & McKee (1989) and Lepp & Shull (1983), also shown in Fig. A1, differ significantly from that computed in this work especially in the low-density limit, at both low and high temperatures (see discussion in Martin et al. 1996).

In considering the cooling by H_2 it is important not to neglect the effect of reactive collisions of H_2 with H or H^+ that cause ortho–para interchange and lead to a ratio out of the equilibrium value 3:1. Calculations of the relative collisional coefficients have been made for H_2–H^+ by Dalgarno et al. (1973) and Flower & Watts (1984), and for H_2–H by Sun & Dalgarno (1994). In the conditions of the primordial gas with $H^+/H \gtrsim 10^{-4}$ the ortho–para exchange is dominated by collisions with protons, and cooling at low temperatures may occur primarily through the $J = 2 \rightarrow 0$ transition of para-H_2. A complete calculation of the cooling function should take into account this effect that has been neglected in the results presented in this section.

A.2. HD

Due to its small dipole moment, $D = 8.3 \times 10^{-4}$ debyes (Abgrall et al. 1982), the energy spacing of the rotational levels of HD is quite large. The energy levels and the rotational radiative transition probabilities have been computed by Dalgarno & Wright (1972) from the experimental data of Trefler & Gush (1968). The calculations have been extended by Abgrall et al. (1982), who considered both dipole and quadrupole transitions and included a large number of rotational and vibrational levels.

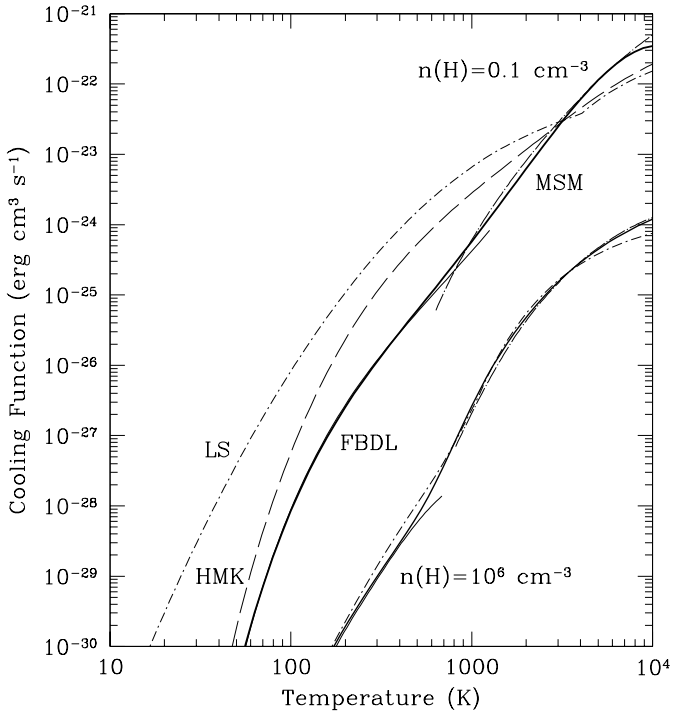

Fig. A1. Cooling function of H_2 for H-H_2 collisions for two values of the density. The thick solid curves show the results of our fit as given by Eqs. A5–A7. The other curves give the cooling functions computed by Lepp & Shull (1983) (LS: dot-dash), Hollenbach & McKee (1989) (HMK: dash), Martin et al. (1996) (MSM: dot-long dash), and Forrey et al. (1997) (FBDL) (thin solid).

Table A3. HD-He Collisional De-excitation Coefficients (from Schaefer 1990)

J'	J	a_0	a_1	α
1	0	4.4×10^{-12}	3.6×10^{-13}	0.77
2	1	4.1×10^{-12}	2.1×10^{-13}	0.92
2	0	3.4×10^{-13}	1.1×10^{-14}	1.10
3	2	2.4×10^{-12}	8.7×10^{-14}	1.03
3	1	3.2×10^{-13}	1.3×10^{-15}	1.47

The two sets of results differ by a factor of two, and we have used the most recent determination.

The coefficients for inelastic scattering of He-HD have been computed by Green (1974) using the Shafer & Gordon (1973) potential of H_2-He, and more recently by Schaefer (1990) with the Schaefer & Köhler (1989) potential at temperatures $T_{\rm g} \leq 600$ K for $0 \leq J \leq 3$ and $\Delta J = +1, +2$. De-excitation coefficients depend approximately linearly with temperature. We have fitted the numerical data of Schaefer (1990) with expressions of the form $\gamma_{J'J} = a_0 + a_1 \ T_{\rm g}^{\alpha}$, and fit coefficients are tabulated in Table A3. These values should be divided by 1.27 to account for the difference between the (HD, H) and (HD, He) interaction potentials (Wright & Morton 1979).

A.3. A total cooling function for the primordial gas

In Fig. A2 we summarize the different contributions to the cooling of a gas of primordial composition. Although the curves have been obtained in the limits $n(\mathrm{H}) \to 0$, they are valid for $n(\mathrm{H}) \lesssim 10^2$ cm^{-3}. At larger densities, the cooling functions rapidly approach the corresponding LTE values; at intermediate densities, the formula (A5) represents a very good approximation. The cooling functions for H-H_2 and H-HD are obtained as described in this work, the H-LiH cooling function is computed according to the prescriptions given by Bougleux & Galli (1997), the cooling function for collisions of H_2^+ with H and e^- was computed by Suchkov & Shchekinov (1978).

The cooling function of HD in the low-density limit for $T_\mathrm{g} \lesssim 10^3$ K is accurately reproduced by the expression

$$\Lambda_\mathrm{HD}[n(\mathrm{H}) \to 0] = 2\gamma_{10}E_{10}\exp(-E_{10}/kT_\mathrm{g}) + (5/3)\gamma_{21}E_{21}\exp(-E_{21}/kT_\mathrm{g}), \quad \text{(A8)}$$

where $E_{10} = 128k$, $E_{21} = 255k$, and the $\gamma_{JJ'}$ are given in Table A3. As for LiH, the cooling function in the low-density limit is well approximated by the polynomial expression $\log\Lambda_\mathrm{LiH}(n\mathrm{H} \to 0) = c_0 + c_1(\log T_\mathrm{g}) + c_2(\log T_\mathrm{g})^2 + c_3(\log T_\mathrm{g})^3 + c_4(\log T_\mathrm{g})^4$ in the temperature range 10–10^3 K. With Λ_LiH in erg cm^3 s^{-1}, the fit coefficients are $c_0 = -31.47$, $c_1 = 8.817$, $c_2 = -4.144$, $c_3 = 0.8292$, $c_4 = -0.04996$.

In the standard model, the radiation temperature is higher than the matter temperature and molecules are a net heating source for the gas. Molecular hydrogen dominates the heating of the gas at temperatures higher than ~ 150 K, whereas HD dominates at lower temperatures. The ability of HD to heat/cool a gas when H_2 molecules become unefficient is a remarkable property of a gas of primordial composition, and has been verified in a number of studies (Varshalovich & Khersonskii 1977, Shchekinov 1986, Bougleux & Galli 1997, Puy & Signore 1997).

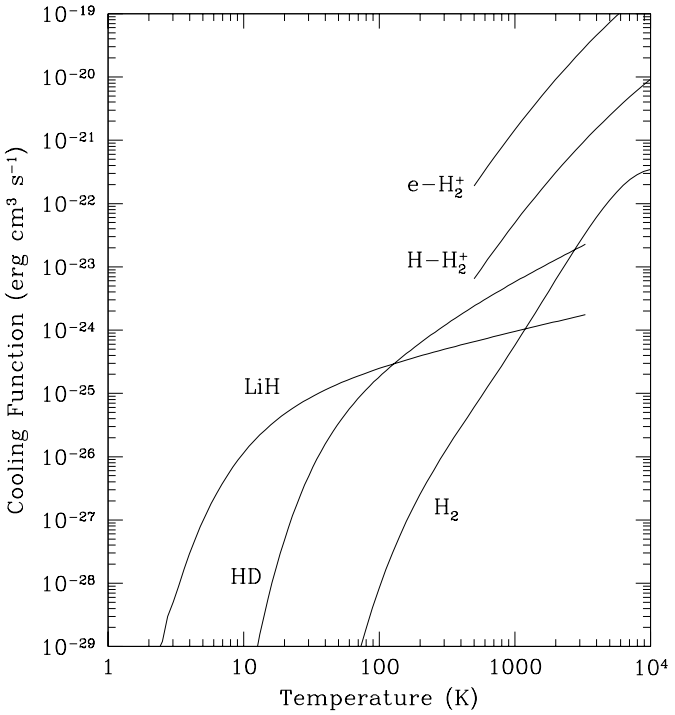

Fig. A2. Cooling function per molecule of H_2, HD, LiH and H_2^+ in the low density limit ($n(\mathrm{H}) \lesssim 10^2$ cm^{-3}).

References

Abel T., Anninos P., Zhang Y., Norman M., 1997, New Astr. 2, 181
Abgrall H., Roueff E., Viala Y., 1982, A&AS 50, 505
Adams N.G., Smith D., 1981, ApJ 248, 373
Adams N.G., Smith D., 1985, ApJ 294, L63
Anninos P., Zhang Y., Abel T., Norman M.L., 1997, New Astr. 2, 209
Argyros J.D., 1974, J. Phys. B 7, 2025
Bates D.R., Opik U., 1968, J. Phys. B 1, 543
Bieniek R.J., 1980, J. Phys. B. 13, 4405
Black J.H., 1978, ApJ 222, 125
Black J.H., 1991, in Molecular Astrophysics, Hartquist, T.W. (ed.), Cambridge Univ. Press, p. 473
Bonifacio P., Molaro P., 1997, MNRAS 285, 847
Boothroyd A.I., Keogh W.J., Martin P.G., Peterson M.R., 1991, J. Chem. Phys. 95, 4343
Boothroyd A.I., Keogh W.J., Martin P.G., Peterson M.R., 1996, J. Chem. Phys. in press
Boreiko R.T., Betz A.L., 1993, ApJ 405, L39
Bougleux E., Galli D., 1997, MNRAS 288, 638
Browne J.C., Dalgarno A. 1969, J. Phys. B 2, 885
Culhane M., McCray R., 1995, ApJ 455, 335
Corrigan S.J.B., 1965, J. Chem Phys. 43, 4381
Dalgarno A., Lepp S., 1987, in IAU Symp. 118, Astrochemistry, M.S. Vardya, S.P. Tarafdar (eds.), Reidel, p. 109
Dalgarno A., Wright E.L., 1972, ApJ 174, L49
Dalgarno A., Black J.H., Weisheit J.C. 1973, Astrophys. Lett. 65, 435
Dalgarno A., Kirby K., Stancil P.C., 1996, ApJ 458, 397
Datz S., Larsson, M., Stromholm, C. et al. 1995, Phys. Rev. A. 52, 2901
de Jong T., 1972, A&A 20, 263
Dubrovich V.K., 1993, SvA Lett. 19, 53
Dubrovich V. K., Lipovka A.A., 1995, A&A 296, 301
Duley W. W., Williams D. A., 1984, Interstellar Chemistry, Academic Press
Dunn G.H., 1968, Phys. Rev. 172, 1
Fehsenfeld F.C., Dunkin D.B., Ferguson E.E., Albritton D.L., 1973, ApJ 183, L25
Flower D.R., 1997a, MNRAS 288, 627
Flower D.R., 1997b, J. Phys. B 30, 1
Flower D.R., Roueff E., 1979, A&A 72, 361
Flower D.R., Watts G.D., 1984, MNRAS 209, 25
Forrey R.C., Balakrishnan N., Dalgarno A., Lepp S., 1997, ApJ 489, 100
Galli D., Palla F., Ferrini F., Penco U., 1995, ApJ 443, 536
Gerlich D., 1982, in Symp. on Atomic and Surface Physics, W. Lindinger, F. Howorka, T. D. Märk, F. Egger (eds.), Dordrecht, p. 304
Gerlich D., Horning S., 1992, Chem. Rev. 92, 1509
Gianturco F. A., Gori Giorgi P., 1996a, ApJ 479, 560
Gianturco F. A., Gori Giorgi P., 1996b, Phys. Rev. A 54, 1
Giroux M.L., Shapiro P.R., 1996, ApJS 102, 191
Grachev S.I., Dubrovich V.K., 1991, Astrophysics 34, 124
Green S., 1974, Physica 76, 609
Green S., Truhlar D.G., 1979, ApJ 231, L101

Henchmann M.J., Adams N.G. , Smith D., 1981, J. Chem. Phys. 75, 1201
Herbst E., 1982, A&A 111, 76
Hollenbach D., McKee C.F., 1979, ApJS 41, 555
Hollenbach D., McKee C.F., 1989, ApJ 342, 306
Holliday M.G., Muckerman J.T. , Friedman L., 1971, J. Chem. Phys. 54, 1058
Janev R.K., Radulović Z.M., 1978, Phys. Rev. A 17, 889
Janev R.K., Langer W.D., Evans K., Post D.E., 1987, Elementary Processes in Hydrogen-Helium Plasmas, Springer
Jones B.J.T. , Wyse R.F.G., 1985, A&A 149, 144
Karpas Z., Anicich V., Huntress W.T., 1979, J. Chem. Phys. 70, 2877
Khersonskii V.K., 1986, Astrophysics 24, 114
Kimura M., Lane N.F., Dalgarno A., Dixson R.G., 1993, ApJ 405, 801
Kimura M., Dutta C., Shimakura N., 1994, ApJ 430, 435 (errata corrige: 1995, ApJ 454, 545)
Krolik J.H., 1990, ApJ 353, 21
Kulander K. , Heller E.J., 1978, J. Chem Phys. 69, 2439
Larsson M., Lepp, S., Dalgarno, A. et al., 1996, A&A 309, L1
Latter W.B., Black J.H., 1991, ApJ 372, 161
Launay J.M., Le Dourneuf M., Zeippen C.J., 1991, A&A 252, 842
Lepp S., Shull J.M., 1983, ApJ 270, 578
Lepp S., Shull J.M., 1984, ApJ 280, 465
Lepp S., Buch V., Dalgarno A., 1995, ApJS, 98, 345
Mandy M. E., Martin P.G., 1993, ApJS 86, 199
Maoli R., Melchiorri F., Tosti D., 1994, ApJ 425, 372
Martin P.G., Schwarz D.H., Mandy M.E., 1996, ApJ, 461 265
Mather J.C., Cheng, E.S., Cottingham, D.A. et al. 1994, ApJ 420, 439
Millar T.J., Bennett A., Herbst E., 1989, ApJ 340, 906
Mitchell G.F., Deveau T.J., 1983, ApJ 266, 646
Moseley J., Aberth W., Peterson J.A., 1970, Phys. Rev. Lett. 24, 435
Ohmura T., Ohmura H., 1960, Phys. Rev. 118, 154
Orient O.J., 1997, Chem. Phys. Lett. 52, 264
Osterbrock D.E., 1989, Astrophysics of Gaseous Nebulae and Active Galactic Nuclei, University Science Books, p. 36
ONeil S.V., Reinhardt W.P., 1978, J. Chem. Phys. 69, 2126
Palla F., Galli D., Silk J., 1995, ApJ 451, 44
Partridge H., Bauschlichert C.W., Stallcop J.R., Levin E., 1993, J. Chem. Phys. 99, 5951
Peart B., Hayton D.A., 1994, J. Phys. B 27, 2551
Peebles P.J.E., Dicke R.H., 1968, ApJ 154, 891
Peterson J.A., Aberth W.H., Moseley J.T., Sheridan J.R., 1971, Phys. Rev. A 3, 1651
Posen A.G., Dalgarno A., Peek J.M., 1983, Atomic Data & Nucl. Data 28, 265
Poulaert G., Brouillard F., Claeys W., McGowan J. W., Van Wassenhove G., 1978, J. Phys. B 11, L671
Puy D., Signore M., 1997, New Astr. 2, 299
Puy D., Alecian G., Le Bourlot J., Léorat J., Pineau des Fôrets G., 1993, A&A 267, 337
Ramaker D.E., Peek J.M., 1976, Phys. Rev. A 13, 58
Ramsbottom C.A., Bell K.L., Berrington K.A., 1994, J. Phys. B. 27, 2905
Rawlings J.M.C., Drew J.E., Barlow M.J. 1993, MNRAS 265, 968
Roberge W., Dalgarno A., 1982, ApJ 255, 489
Sasaki S., Takahara F., 1993, PASJ 45, 655
Saslaw W.C., Zipoy D., 1967, Nat 216, 967
Schaefer J., 1990, AAS 85, 1101
Schaefer J., Köhler W.E., 1989, Z.f.Phys. 13, 217
Schmeltekopf A.L, Fehsenfeld F.C., Ferguson E.E., 1967, ApJ 118, L155
Schneider I.F., Dulieu O., Giusti-Suzor A., Roueff E., 1994, ApJ 424, 983 (errata in ApJ 486, 580)
Schulz G.J., Asundi R.K., 1967, Phys. Rev. 158, 25
Shafer R., Gordon R.G., 1973, J. Chem. Phys. 58, 542
Shapiro P.R., 1992, in Astrochemistry of Cosmic Phenomena, IAU Symp. 150, P.D. Singh (ed.), Kluwer Acad. Publ., p.73
Shapiro P.R., Kang H., 1987, ApJ 318, 32
Shavitt I., 1959, J. Chem. Phys. 31, 1359
Shchekinov Yu. A., 1986, SvA Lett. 12, 211
Shull J.M., Beckwith S., 1982, ARA&A 20, 163
Sidhu K.S., Miller S., Tennyson J., 1992, A&A 255, 453
Smith D., Adams N.G., Alge E., 1982, ApJ 263, 123
Smith M.S., Kawano L.H., Malaney R.A., 1993, ApJS 85, 219
Stancil P.C., 1994, ApJ 430, 360
Stancil P.C., Zygelman B., 1996, ApJ 472, 102
Stancil P.C., Dalgarno A., 1997, ApJ 479, 543
Stancil P.C., Babb J.F., Dalgarno A., 1993, ApJ 414, 672
Stancil P.C., Lepp S., Dalgarno A., 1996, ApJ 458, 401
Stromhölm C., Schneider I. F., Sundström G. et al., 1995, Phys. Rev. A 52, R4320
Suchkov A.A., Shchekinov Yu. A., 1978, SvA Lett. 4, 164
Sundström G., Mowat, J.R., Danared, H. et al., 1994, Science 263, 785
Sun Y., Dalgarno A., 1994, ApJ 427, 1053
Tegmark M., Silk J., Rees M.J., et al. 1997, ApJ 474, 1
Theard L.P., Huntress W.T., 1974, J. Chem. Phys. 60, 2840
Trefler M., Gush H.P., 1968, Phys. Rev. Lett. 20, 703
Turner J., Kirby-Docken K., Dalgarno A., 1977, ApJS 35, 281
Truhlar D.G., Horowitz C.J., 1978, J. Chem. Phys. 68, 2466
Tytler D., Burles S., 1997, in Origin of Matter & Evolution of Galaxies, Kajino, T., Kubono, S., Yoshii, Y. (eds.), World Scientific, p. 37
van den Bergh S., 1989, A&AR 1, 111
Varandas A.J.C., Brown F.B., Mead C.A., Thrular D.G., Blais N.G., 1987, J. Chem. Phys. 86, 6258
Varshalovich D.A., Khersonskii V.K., 1977, SvA Lett. 2, 227
Verner D.A., Ferland G.J., 1996, ApJS 103, 467
von Busch F., Dunn G.H., 1972, Phys. Rev. A 5, 1726
Watson W.D., Christensen R.B., Deissler R.J., 1978, A&A 69, 159
Wishart A.W., 1979, MNRAS 187, 59p
Wright E.L., Morton D.C., 1979, ApJ 227, 483
Yousif F.B., Mitchell J.B.A., 1989, Phys. Rev. A 40, 4318
Zhang J.Z.H., Miller W.H., 1989, J. Chem Phys. 91, 1528
Zygelman B., Dalgarno A., 1990, ApJ 365, 239
Zygelman B., Dalgarno A., Kimura M., Lane N.F., 1989, Phys. Rev. A 40, 2340